



HAL
open science

The genetic architecture of recombination rates is polygenic and differs between the sexes in wild house sparrows (*Passer domesticus*)

John Mcauley, Bertrand Servin, Hamish Burnett, Cathrine Brekke, Lucy Peters, Ingerid Hagen, Alina Niskanen, Thor Harald Ringsby, Arild Husby, Henrik Jensen, et al.

► To cite this version:

John Mcauley, Bertrand Servin, Hamish Burnett, Cathrine Brekke, Lucy Peters, et al.. The genetic architecture of recombination rates is polygenic and differs between the sexes in wild house sparrows (*Passer domesticus*). *Molecular Biology and Evolution*, 2024, 41 (9), 10.1093/molbev/msae179 . hal-04681764v1

HAL Id: hal-04681764

<https://hal.inrae.fr/hal-04681764v1>

Submitted on 2 Sep 2024 (v1), last revised 20 Sep 2024 (v2)

HAL is a multi-disciplinary open access archive for the deposit and dissemination of scientific research documents, whether they are published or not. The documents may come from teaching and research institutions in France or abroad, or from public or private research centers.

L'archive ouverte pluridisciplinaire **HAL**, est destinée au dépôt et à la diffusion de documents scientifiques de niveau recherche, publiés ou non, émanant des établissements d'enseignement et de recherche français ou étrangers, des laboratoires publics ou privés.



Distributed under a Creative Commons Attribution - NonCommercial 4.0 International License

1 **The genetic architecture of recombination rates is polygenic and differs between**
 2 **the sexes in wild house sparrows (*Passer domesticus*).**

3
 4 **John B. McAuley¹, Bertrand Servin², Hamish A. Burnett³, Cathrine Brekke¹, Lucy Peters²,**
 5 **Ingerid J. Hagen^{3,4}, Alina K. Niskanen^{3,5}, Thor Harald Ringsby³, Arild Husby⁶, Henrik Jensen³,**
 6 **Susan E. Johnston^{1,*}**

7 ¹ Institute of Ecology and Evolution, School of Biology, University of Edinburgh, Edinburgh EH9 3FL,
 8 United Kingdom.

9 ² GenPhySE, Université de Toulouse, INRAE, ENVT, 31326 Castanet Tolosan, France.

10 ³ Centre for Biodiversity Dynamics, Department of Biology, Norwegian University of Science and
 11 Technology, 7491 Trondheim, Norway.

12 ⁴ Norwegian Institute for Nature Research, 7034 Trondheim, Norway

13 ⁵ Ecology and Genetics Research Unit, University of Oulu, 90014 Oulu, Finland.

14 ⁶ Evolutionary Biology, Department of Ecology and Genetics, Uppsala University, 75236 Uppsala,
 15 Sweden.

16 * Corresponding author: Susan.Johnston@ed.ac.uk

17
 18 **Abstract**

19 Meiotic recombination through chromosomal crossing-over is a fundamental feature of sex and an
 20 important driver of genomic diversity. It ensures proper disjunction, allows increased selection responses,
 21 and prevents mutation accumulation; however, it is also mutagenic and can break up favourable
 22 haplotypes. This cost/benefit dynamic is likely to vary depending on mechanistic and evolutionary
 23 contexts, and indeed, recombination rates show huge variation in nature. Identifying the genetic
 24 architecture of this variation is key to understanding its causes and consequences. Here, we investigate
 25 individual recombination rate variation in wild house sparrows (*Passer domesticus*). We integrate
 26 genomic and pedigree data to identify autosomal crossover counts (ACC) and intra-chromosomal allelic
 27 shuffling (\bar{r}_{intra}) in 13,056 gametes transmitted from 2,653 individuals to their offspring. Females had
 28 1.37 times higher ACC, and 1.55 times higher \bar{r}_{intra} than males. ACC and \bar{r}_{intra} were heritable in
 29 females and males (ACC $h^2 = 0.23$ and 0.11 ; \bar{r}_{intra} $h^2 = 0.12$ and 0.14), but cross-sex additive genetic
 30 correlations were low ($r_A = 0.29$ and 0.32 for ACC and \bar{r}_{intra}). Conditional bivariate analyses showed that
 31 all measures remained heritable after accounting for genetic values in the opposite sex, indicating that
 32 sex-specific ACC and \bar{r}_{intra} can evolve somewhat independently. Genome-wide models showed that
 33 ACC and \bar{r}_{intra} are polygenic and driven by many small-effect loci, many of which are likely to act in
 34 *trans* as global recombination modifiers. Our findings show that recombination rates of females and males

1 can have different evolutionary potential in wild birds, providing a compelling mechanism for the evolution
2 of sexual dimorphism in recombination.

3 **Introduction**

4 Meiotic recombination via chromosomal crossing-over is an essential process in sexual reproduction and
5 has a key role in generating diversity in eukaryotic genomes (Coop and Przeworski 2007). Crossing-over
6 can be beneficial: it ensures proper segregation of chromosomes (Koehler et al. 1996), prevents the
7 accumulation of deleterious alleles, and increases the speed at which populations can respond to
8 selection (Hill and Robertson 1966; Felsenstein 1974; Otto and Lenormand 2002). On the other hand,
9 recombination can increase the risk of mutations at DNA double-strand break sites (Halldorsson et al.
10 2019; Hinch et al. 2023), and can break down favourable allele combinations previously built up by
11 selection (Charlesworth and Barton 1996). Despite these trade-offs, there is extensive variation in
12 recombination rate both within and between chromosomes, individuals, populations, sexes, and species
13 (Myers et al. 2005; Coop and Przeworski 2007; Ritz et al. 2017; Stapley et al. 2017). The cost-benefit
14 dynamic of recombination rate is likely to vary depending on mechanistic and evolutionary contexts, and if
15 rates are heritable (i.e., there is underlying additive genetic variation), then they have the potential to
16 respond to selection. Therefore, understanding the genetic basis of recombination rate variation - that is,
17 the amount of additive genetic variation and the effect sizes and distributions of gene variants that
18 contribute to such variation - is a critical first step in determining if and how they are contributing to
19 adaptation, and how they themselves are evolving (Ritz et al. 2017; Stapley et al. 2017).

20
21 To date, studies investigating the genetic basis of recombination rate variation have mostly been limited
22 to model systems and livestock and have demonstrated that crossover rates can be heritable and
23 associated with particular genetic variants (Cirulli et al. 2007; Smukowski and Noor 2011; Cattani et al.
24 2012; Chan et al. 2012; Kong et al. 2014; Hunter et al. 2016; Johnston et al. 2016; Kadri et al. 2016; Petit
25 et al. 2017; Johnston et al. 2018; Weng et al. 2019; Samuk et al. 2020; Johnsson et al. 2021; Brekke,
26 Johnston, et al. 2022; Brekke et al. 2023). In some systems such as mammals, the genetic architecture
27 can be oligogenic, with loci with meiotic functions being repeatedly implicated (e.g. *RNF212*, *RNF212B*,
28 *MEI1*, *MSH4*, *PRDM9*); whereas in other systems, such as Atlantic salmon, variation can be polygenic
29 (i.e., controlled by many loci of small effect). Nevertheless, the patterns observed in these studies may
30 not be generalisable to other systems due to a number of specific factors, such as: relatively low
31 individual variation in recombination rates (e.g. in *Drosophila spp.*); long-periods of female meiotic arrest
32 (e.g. in humans; (MacLennan et al. 2015); dynamic variation in karyotype that can affect crossover
33 distributions (e.g. in mice; (Capilla et al. 2014; Garagna et al. 2014); and a history of strong and sustained
34 directional selection, which theoretically imposes indirect selection for increased recombination in small
35 populations (e.g. in crops and livestock; (Otto and Barton 2001; Ross-Ibarra 2004); but see (Muñoz-
36 Fuentes et al. 2015). Another consideration is that in many vertebrates, the positioning of recombination
37 hotspots is determined by *PRDM9*, a gene coding for a zinc finger protein that binds to particular

1 sequence motifs in the genome to initiate double strand breaks (Baudat et al. 2010; Baker et al. 2017). As
2 double strand break repair is mutagenic (Hinch et al. 2023), this can erode the recognised motifs and
3 reduce the number of binding sites, which may in turn select for novel *PRDM9* zinc finger alleles and a
4 corresponding rapid turnover of hotspots (Myers et al. 2010; Grey et al. 2018). Indeed, *PRDM9* is one of
5 the fastest evolving genes in species where it is functional, but it has also been lost from clades such as
6 birds, canids and amphibians, where recombination hotspots appear to be stable and enriched at
7 functional elements (Singhal et al. 2015; Baker et al. 2017). Therefore, research in both non-model, non-
8 *PRDM9*, and non-mammalian systems is required to better understand the genetic architecture of
9 recombination rate more broadly, and how it is affected by other intrinsic and extrinsic variation in natural
10 environments.

11
12 A near-universal feature of recombination is that rates and landscapes differ in their degree and
13 magnitude between male and female gametes, a phenomenon known as “heterochiasmy” (Lenormand
14 and Dutheil 2005; Sardell and Kirkpatrick 2020). Numerous hypotheses have been proposed to explain
15 how it has evolved, including: reducing or increasing crossing-over in the sex under stronger selection
16 (Trivers 1988; Burt et al. 1991); gametic selection reducing crossovers in the sex with stronger haploid
17 selection (Nei 1969; Lenormand 2003; Lenormand and Dutheil 2005); counteracting the effects of meiotic
18 drive (Brandvain and Coop 2012); or that it has arisen through drift (Burt et al. 1991). Yet despite several
19 comparative investigations of overall rate (Lenormand and Dutheil 2005; Mank 2009; Cooney et al. 2021),
20 there remains little empirical support for these hypotheses. Interestingly, some of the empirical studies
21 above show that the genetic architecture of recombination rate can differ between the sexes, in terms of
22 the large effect loci underpinning them (Kong et al. 2014; Johnston et al. 2016; Johnston et al. 2018;
23 Brekke, Berg, et al. 2022; Brekke, Johnston, et al. 2022), and/or their cross-sex additive genetic
24 correlations being significantly less than one (Johnston et al. 2016; Brekke et al. 2023). Therefore, studies
25 that specifically dissect within and between-sex genetic architectures in diverse species are imperative to
26 gain a full understanding on the molecular mechanisms and evolutionary drivers/constraints contributing
27 to both recombination rate variation and heterochiasmy from the chromosomal to species levels.

28
29 Avian systems present a unique opportunity for further developing our understanding of the genetic basis
30 of recombination rate variation and heterochiasmy in the wild. Linkage mapping and cytogenetic studies
31 in birds have shown that despite relatively conserved karyotypes, there is substantial variation in
32 recombination rates, broad-scale landscapes, and heterochiasmy (Figure 1; see Table S1 for a full list of
33 references). In addition, birds lack *PRDM9* and have highly conserved, stable recombination hotspots that
34 are enriched at transcription start sites (TSS) and gene promoter regions, likely due to increased
35 chromatin accessibility (Pan et al. 2011; Singhal et al. 2015; Kawakami et al. 2017; Bascón-Cardozo et al.
36 2022). A number of wild bird populations have been subject to long-term, individual based studies of their
37 ecology and evolution. As genomic and pedigree data for these populations proliferates, this presents an

1 opportunity to investigate recombination in wild, non-model systems, and ultimately, the relationships
2 between recombination rates, their genetic architectures, and individual fitness components such as
3 reproduction and offspring viability (Johnston et al. 2022).

5 **Figure 1:** Phylogeny of birds where within-sex recombination rates have been estimated using linkage
6 mapping or cytogenetic analysis of chiasma counts. Chiasma count estimates are indicated with asterisks
7 (*). The underlying data is provided in Table S1 using data compiled in (Malinovskaya, Tishakova, et al.
8 2020) and other sources. The phylogeny was obtained from TimeTree v5 (Kumar et al. 2022). This figure
9 should be taken as illustrative only - some of the linkage map data is likely to have had poor marker
10 densities in telomeric regions and have less resolution to detect double crossovers. As recombination
11 landscape and crossover rates are sex-dependent, this could underestimate recombination in one sex,
12 hence why we have not made a formal comparison. **References:** (Pigozzi and Solari 1998; Pigozzi 2001;
13 Hansson et al. 2005; Calderón and Pigozzi 2006; Backström et al. 2008; Stapley et al. 2008; Groenen et
14 al. 2009; Jaari et al. 2009; Aslam et al. 2010; Hansson et al. 2010; Kawakami et al. 2014; van Oers et al.
15 2014; Torgasheva and Borodin 2017; Weng et al. 2019; Malinovskaya, Tishakova, et al. 2020; Peñalba et
16 al. 2020; Robledo-Ruiz et al. 2022).

17
18 Here, we examine sex-specific variation in individual autosomal recombination rate and its genetic
19 architecture in a wild meta-population of house sparrows (*Passer domesticus*). House sparrows are small
20 passerine birds native to Eurasia, and are now distributed across most human-habited areas of the world.
21 They are human commensals, often found in cities and farmland, and their ubiquity makes them a model
22 system for ecology, evolution and adaptation (Anderson 2006). House sparrows in the Helgeland
23 archipelago have relatively low dispersal from their natal island (Saatoglu et al. 2021), allowing for
24 detailed data on survival and reproduction to be collected since 1993 (Jensen et al. 2004; Stubberud et
25 al. 2017; Araya-Ajoy et al. 2021). This population has extensive genomic resources, including an
26 annotated reference genome (Elgvin et al. 2017), a 6.5K SNP linkage map (Hagen et al. 2020), high-
27 density SNP arrays (Lundregan et al. 2018) and a dense genetic pedigree (Niskanen et al. 2020). In this
28 study, we characterise individual recombination rates using SNP and pedigree data, focussing on
29 autosomes to allow a direct comparison between recombination in the same genome within each sex. We
30 investigate: (a) how recombination varies at the broad scale across chromosomes; (b) the additive
31 genetic variance and genetic architecture of individual recombination rates; and (c) how these factors
32 vary between the sexes, including the potential for female and male rates to evolve independently.

34 Results

35 Linkage mapping.

36 Autosomal linkage maps were constructed using data from 1,320 full-sib families, incorporating linkage
37 information from 9,777 gametes transmitted by 1,805 individuals to their offspring. We mapped 56,765
38 autosomal SNPs of known position relative to the house sparrow genome *Passer_domesticus*-1.0 to
39 45,022 unique centiMorgan (cM) positions on 28 autosomes, with heterogeneity in the landscape of

1 recombination within and between the sexes (Figures S1 and S2, Tables S2 and S3). The female and
 2 male autosomal maps were 1994.4 cM (2.18 cM/Mb) and 1627.2 cM (1.78 cM/Mb), respectively. The
 3 female map length was 1.23 times longer than the male map length. There was a strong correlation
 4 between chromosome length and genetic map length in each sex ($r^2 = 0.97$ and 0.96 for females and
 5 males, respectively; $P < 0.001$) and recombination rates were female-biased for most chromosomes
 6 (Figure 2A). Chromosome-wide recombination rate (cM/Mb) was higher on smaller autosomes ($r^2 =$
 7 0.749 , $P < 0.0001$, fitted as a logarithmic function), with micro-chromosomes demonstrating
 8 recombination rates 3 to 5 times that of the genome-wide average (Figure 2B). Despite their high
 9 recombination rates, chromosomes 21, 22, 25, 27 and 28 still had linkage map lengths much shorter than
 10 the expectation of 50 cM, indicating that the obligate crossover was not always sampled on those
 11 chromosomes with the current genomic dataset. Summary statistics for map lengths are provided in Table
 12 S2, and the full sex-specific linkage maps are provided in Table S3.

13

14 **Figure 2.** Variation in recombination rates between chromosomes, showing correlations between (A) the
 15 sex-specific linkage map lengths (cM) and chromosome length (Mb); and (B) sex-specific chromosomal
 16 recombination rate (cM/Mb) and chromosome length. Numbers are individual chromosomes, and lines
 17 and the grey-shaded areas indicate the regression slopes and standard errors, respectively.
 18 Chromosome 25 has been omitted from Figure 2B due to its exceptionally high recombination rate (30
 19 cM/Mb and 26.9 cM/Mb in females and males, respectively).

20

21 Identification of meiotic crossovers.

22 We used the full pedigree of 12,959 genotyped individuals to phase chromosomes infer crossover (CO)
 23 positions in gametes transmitted from focal individuals (FIDs) to their offspring. In total, we identified
 24 236,671 COs in 13,054 phased genotypes from 6,409 gametes transmitted from 1,354 unique female
 25 FIDs and 6,647 gametes transmitted from 1,299 unique male FIDs. Larger chromosomes had more COs
 26 per gamete than small chromosomes, with chromosomes 1 and 2 having up to 8 COs per gamete in
 27 some rare cases in both sexes (Figure 3, Figure S3). Chromosomes 10 to 20 generally had 50% non-
 28 recombinant chromosomes, likely reflective of crossover interference over these short chromosomes
 29 leading to a single obligate CO, which has a 50% chance of segregation into the gamete. Chromosomes
 30 21 to 28 had more than 50% of chromosomes with no COs, meaning that we had low power to pick up
 31 COs on these chromosomes; these chromosomes were discarded from estimates of genome-wide
 32 recombination rates.

33 **Figure 3:** Distribution of crossover (CO) counts per chromosome as the proportion of total number of
 34 gametes ($N = 13,054$). The white dashed line is the minimum expected proportion of gametes with 0 COs
 35 per chromosome due to obligate crossing-over and Mendelian segregation of COs into gametes.
 36 Separate plots for each sex are provided in Figure S3.

37

1
2 **Individual recombination rate variation**

3 The crossover dataset (for chromosomes 1 to 20 and 1A) was used to calculate recombination rates in
4 each gamete using two measures: the total autosomal crossover count (ACC), and the rate of intra-
5 chromosomal allelic shuffling (\bar{r}_{intra}), which is the probability that two randomly chosen SNP loci on the
6 same chromosome are uncoupled by a crossover during meiosis (Veller et al. 2019). In contrast to ACC,
7 \bar{r}_{intra} accounts for the effect of crossover positioning, where crossovers located toward the centre of a
8 chromosome will lead to higher shuffling than crossovers located at chromosome ends. The mean ACC
9 was 1.37 times higher in females than in males, with mean ACCs of 18.9 and 13.8, respectively (Figure
10 4). The mean rate of intra-chromosomal shuffling \bar{r}_{intra} was 1.55 times higher in females (Figure 4). ACC
11 and \bar{r}_{intra} were positively correlated ($r^2 = 0.684$, $P < 0.0001$; Figure S4A).

13 **Figure 4.** Distributions of female and male recombination rates in gametes transmitted from FIDs to their
14 offspring for A) ACC (autosomal crossover count); and B) \bar{r}_{intra} , (rate of intra-chromosomal shuffling).

15
16 **Heritability and genetic correlations of individual recombination rates.**

17 The proportion of phenotypic variance in ACC and \bar{r}_{intra} explained by additive genetic effects (the
18 narrow-sense heritability, h^2) was determined within each sex using an animal model approach fitting a
19 genomic relatedness matrix as a random effect. We also calculated the mean-standardised additive
20 genetic variance for ACC, defined as the evolvability (I_A), which quantifies the expected proportional
21 change per one unit of selection (Hansen et al. 2011). For all models of ACC and \bar{r}_{intra} , only fixed effects
22 of total phase coverage, and total phase coverage² were significant (Table S4), as were the additive
23 genetic, permanent environment (repeated measures) and residual random effects (Table 1).

24
25 ACC was heritable and evolvable in females ($h^2 = 0.232$, $I_A = 0.016$) and males ($h^2 = 0.112$, $I_A = 0.006$, P
26 < 0.001 , Table 1). The cross-sex additive genetic correlation was positive ($r_A = 0.292$, $se = 0.154$), but
27 was not significantly different from zero (χ_1^2 LRT = 3.48, $P = 0.062$) and was significantly lower than one
28 (χ_1^2 LRT = 19.06, $P < 0.001$), indicating that the genetic basis of ACC has a significant unshared
29 component between males and females. This was confirmed when conditioning the within sex ACC on
30 the genetic value in the opposite sex, where female and male ACC remained independently heritable (h^2
31 = 0.126 and 0.077, respectively, $P < 0.001$, Table 1). We also calculated the permanent environment
32 effect, a repeated measures parameter which accounts for constant differences between individuals over
33 an above the heritability (Kruuk 2004). This effect was lower but significant in both females and males
34 ($pe^2 = 0.057$ and 0.077 respectively, $P < 0.05$, Table 1), indicating that ACC is also partially explained by
35 individual differences not attributed to additive genetic effects.

36

1 \bar{r}_{intra} was heritable in females and males ($h^2 = 0.116$ & 0.140 , respectively, $P < 0.001$, Table 1); as this
 2 metric is on the absolute scale, evolvabilities cannot be calculated (see (Hansen et al. 2011). When
 3 corrected for ACC by adding it as an additional fixed covariate, heritabilities were reduced but remained
 4 significant ($h^2 = 0.042$ & 0.084 respectively, $P < 0.001$). The cross-sex additive genetic correlation of ACC
 5 was positive ($r_A = 0.319$, $se = 0.151$) and was significantly different from zero (χ_1^2 LRT = 4.54 , $P = 0.033$)
 6 and one (χ_1^2 LRT = 23.21 , $P < 0.001$), again indicating that the genetic basis of \bar{r}_{intra} has an unshared
 7 component between males and females. This was confirmed when conditioning the within-sex \bar{r}_{intra} on
 8 the genetic value in the opposite sex, where female and male \bar{r}_{intra} were independently heritable ($h^2 =$
 9 0.082 and 0.077 , respectively, $P < 0.001$, Table 1). There was a significant permanent environment effect
 10 for \bar{r}_{intra} in males ($pe^2 = 0.049$), but not females (Table 1).

11
 12 For both ACC and \bar{r}_{intra} , we investigated the potential contribution of female-restricted chromosomes
 13 i.e., the germline-restricted chromosome (Borodin et al. 2022) and the W chromosome to phenotypic
 14 variation by fitting individual matriline (i.e., the path of inheritance from mothers to offspring) as an
 15 additional random effect. Matriline did not explain any of the phenotypic variance, indicating that neither
 16 female-restricted chromosomes significantly contributed to variation in recombination rates in this
 17 population. A full explanation of why this analysis was carried out is provided in the Discussion and
 18 Methods sections.

19
 20
 21 **Table 1:** Proportions of phenotypic variance explained by additive genetic (h^2), permanent environment
 22 effect (pe^2) and residual variance (r^2). V_P and V_P (obs) are the phenotypic variances as estimated from the
 23 animal model and from the raw data, respectively. The mean value is from the raw data. I_A is the
 24 evolvability (note that I_A cannot be estimated for \bar{r}_{intra} due to it being on the absolute scale). h^2_{indep} is the
 25 trait heritability independent of the genetic value of the other sex, and r_A is the additive genetic correlation.
 26 Values in parentheses are the standard errors. Significances of h^2 , pe^2 and h^2_{indep} estimates are indicated
 27 by * ($P < 0.05$), ** ($P < 0.001$) and *** ($P < 0.001$). All results are from 6,409 gametes from 1,354 females
 28 and 6,647 gametes from 1,299 males on all crossovers occurring on chromosomes 1A and 1 to 20.

Rate Measure	Sex	V_P	V_P (Obs)	Mean	V_A	h^2	pe^2	I_A	h^2_{indep}	r_A
ACC	F	23.93 (0.56)	24.41	18.92	5.561 (0.761)	0.232 (0.029)***	0.057 (0.023)*	0.016 ($2.13e^{-3}$)	0.126 (0.023)***	0.292 (0.154)
	M	10.76 (0.221)	10.56	13.76	1.202 (0.273)	0.112 (0.025)***	0.077 (0.023)*	$6.35e^{-3}$ ($1.44e^{-3}$)	0.077 (0.019)***	
\bar{r}_{intra}	F	$5.50e^{-5}$ ($1.04e^{-6}$)	$5.56e^{-5}$	0.027	$6.40e^{-6}$ ($7.24e^{-7}$)	0.116 (0.012)***	$1.28e^{-5}$ ($2.43e^{-7}$)	-	0.077 (0.01)***	0.319 (0.151)
	M	$5.77e^{-5}$ ($1.18e^{-6}$)	$5.75e^{-5}$	0.017	$8.07e^{-6}$ ($1.43e^{-6}$)	0.14 (0.027)***	0.049 (0.020)*	-	0.082 (0.019)***	

29
 30

Genome-wide association studies of individual recombination rates.

Genome-wide association studies were carried out using a larger genomic dataset of 65,840 SNPs, including Z-linked SNPs and any SNPs of unknown position relative to the house sparrow genome. These models accounted for repeated measures within the same individuals. We did not identify any loci that were significantly associated with variation in ACC or \bar{r}_{intra} in females or males (Figure 5, Figure S5), with a power analysis indicating that we had 95% power to identify any loci explaining >3.2% of the phenotypic variance. We carried out Empirical Bayes analyses of the GWAS summary statistics to identify loci with significant non-zero effects. For female ACC, 4,696 SNPs (7.13%) and 1,178 SNPs (1.79%) had non-zero effects at the significance thresholds of $\alpha = 0.05$ and 0.01, respectively (Figure S6). For male ACC, 179 SNPs (0.27%) and 7 SNPs (0.01%) had non-zero effects on ACC at the levels of $\alpha = 0.05$ and 0.01, respectively (Figure S6). For female \bar{r}_{intra} , 1213 SNPs (1.84%) and 143 SNPs (0.22%) had non-zero effects at the significance thresholds of $\alpha = 0.05$ and 0.01, respectively (Figure S6). For male \bar{r}_{intra} , 1254 SNPs (1.9%) and 151 SNPs (0.23%) had non-zero effects on ACC at the levels of $\alpha = 0.05$ and 0.01, respectively (Figure S6).

Figure 5: Genome-wide association plots for autosomal crossover count (ACC) and intra-chromosomal shuffling (\bar{r}_{intra}) in females and males at 65,840 SNPs. Phenotypic measures are from 6,409 gametes from 1,354 females and 6,647 gametes from 1,299 males. The dashed line is the genome-wide Bonferroni-corrected significance level (equivalent to $\alpha = 0.05$). Chromosome 0 indicates SNPs of unknown genomic position. Association statistics have been corrected with the genomic control parameter λ . P-P plots of the null expectations of each plot is provided in Figure S5. Note that visually, P values on the Z chromosome appear to be lower than on other chromosomes. This is an artefact of overplotting of much higher marker densities on the other chromosomes, and association statistics are not significantly lower on the Z chromosome.

Chromosome partitioning of additive genetic variance.

To confirm the hypothesis of a polygenic architecture of recombination rates, we used a chromosome partitioning approach estimating the contribution of each chromosome to the phenotypic variance (Yang, Manolio, et al. 2011). We computed separate genomic relatedness matrices for (a) chromosome i and (b) all chromosomes excluding i , and fit both as random effects in an animal model. Larger chromosomes contributed more to the total additive genetic variance for female ACC, female \bar{r}_{intra} , and male \bar{r}_{intra} (linear regression $P < 0.01$, Figure 6, Table S6, Table S7), supporting the hypothesis of a polygenic architecture underpinning these traits. The absence of an effect for male ACC is likely due to a lack of model convergence leading to zero estimates for two of the largest chromosomes, 2 and 3; when removing these two chromosomes, the linear regression was significant ($t = 4.120$, $P < 0.001$, Adjusted $R^2 = 0.5$).

We then modified this approach to determine if the polygenic components underpinning recombination rate are commonly acting in *trans* (i.e., they affect the global recombination rate) rather than *cis* (i.e., they

1 affect the recombination rate on the chromosome on which they are situated, and/or are in linkage
 2 disequilibrium with heritable aspects of chromatin structure that affect local recombination rates). For
 3 each chromosome i , we calculated ACC and \bar{r}_{intra} for chromosomes 1A and 1 to 20 excluding i , and
 4 then reran the animal models and correlations as above. Similarly, larger chromosomes contributed more
 5 to the total additive genetic variance for female ACC, female \bar{r}_{intra} , and male \bar{r}_{intra} (linear regression P
 6 < 0.05 , Figure 6, Table S6, Table S7). These effects were weaker for female \bar{r}_{intra} and male \bar{r}_{intra} when
 7 compared to the full model above, suggesting that a significant component of variation in intra-
 8 chromosomal shuffling may still act in *cis*. However, for female ACC, this effect was highly similar in both
 9 models, indicating that polygenic variation in female autosomal crossover count is likely to be more
 10 commonly acting in *trans* within this population.

11
 12 **Figure 6:** Chromosome partitioning of additive genetic effects on autosomal crossover count (ACC) and
 13 intra-chromosomal shuffling (\bar{r}_{intra}) in females and males. Each point indicates the proportion of
 14 phenotypic variance explained by a chromosome-specific genomic relatedness matrix modelled as a
 15 function of chromosome length. The top row partitions variance for recombination rates estimated on all
 16 chromosomes (1-20 & 1A), which accounts for *cis* and *trans* effects combined. The bottom row partitions
 17 variance for recombination rates excluding that chromosome, accounting for *trans* effects only.
 18 Correlations are analysed with a linear regression (full results in Table S6). Full chromosome partitioning
 19 results are provided in Table S7.

20

21 DISCUSSION

22 In this study, we have shown that female house sparrows have 1.37 times higher autosomal crossover
 23 counts (ACC) and 1.55 times more intra-chromosomal shuffling (\bar{r}_{intra}) than males. ACC was moderately
 24 heritable in both females and males ($h^2 = 0.23$ and 0.11 , respectively), as was \bar{r}_{intra} ($h^2 = 0.12$ and 0.14 ,
 25 respectively). A genome-wide association study found no regions of the genome with a significant effect
 26 on recombination rate, with chromosome partitioning and Empirical Bayes approaches supporting a
 27 polygenic genetic architecture. Larger chromosomes contributed more additive genetic variation to ACC
 28 and \bar{r}_{intra} in the rest of the genome, with further analysis implying that polygenic effects in female ACC
 29 are mostly acting in *trans*, i.e., affecting the global recombination rate. For both ACC and \bar{r}_{intra} , the inter-
 30 sex additive genetic correlation was low ($r_A \sim 0.3$), and both traits remained heritable within each sex after
 31 controlling for the genetic values of the opposite sex, indicating that the genetic architecture can evolve
 32 independently within each sex. Here, we discuss in more detail the mechanisms by which polygenic
 33 architecture is likely to contribute to variation in recombination rate, how this differs between the sexes,
 34 and how the broad scale recombination landscape compares with other studies.

35

36 Sex differences in recombination and its genetic architecture.

37 This study provides a compelling example of heterochiasmy in both recombination rates and the broad-
 38 scale recombination landscapes. More importantly, our study shows that these sex differences are also
 39 underpinned by different genetic architectures. Male and female recombination rates are likely to have

1 some degree of shared genetic architecture, as shown by additive genetic correlations of $r_A \approx 0.3$; whilst
2 there were moderate standard errors around these estimates, this value was significantly lower than 1 for
3 both ACC and \bar{r}_{intra} . Both traits remained heritable within each sex, even after conditioning on genetic
4 values in the opposite sex, with values ranging from $h^2 = 0.077$ to 0.13.

5
6 This indicates that there is potential for evolution of recombination rates within each sex independent of
7 that in the other sex, which could affect the degree and potentially the direction of heterochiasmy within
8 the population. With the exception of domestic chickens (Weng et al. 2019), our study is the largest study
9 of individual variation in recombination in birds, and our study is the largest to investigate sex-specific
10 effects at the individual and population levels. As the number of gametes from males and females are
11 similar in our study, and coverage is high across the chromosomes we analysed here, we are confident
12 that we capture the vast majority of biologically meaningful autosomal COs within each sex. While we
13 cannot directly relate heterochiasmy in a single population to a particular hypothesis outlined in the
14 introduction, our results add to a growing body of data that there is sexual dimorphism in not only the rate
15 of crossing over, but also in its positioning and in its genetic architecture. More broadly, our results
16 suggest that while there are fundamental similarities in recombination between female and male meiosis,
17 the observed differences in our study may indicate some distinct biological processes at work between
18 the sexes. Future studies investigating the evolutionary causes and consequences of recombination
19 should endeavour to consider how sex-differences in meiotic processes contribute to observed variation.

21 **Variation in crossover count and intra-chromosomal shuffling.**

22 Much of the theory proposed to explain the advantages and disadvantages of recombination rate
23 variation centres around the generation and preservation of beneficial haplotypes through shuffling of
24 alleles at linked sites (Hill and Robertson 1966; Felsenstein 1974; Kondrashov 1988). The efficacy and
25 extent to which crossovers shuffle linked alleles within chromosomes is not only a function of CO count,
26 but also of the CO position (Veller et al. 2019). For example, a crossover in close proximity to a
27 chromosome end will lead to much less allele shuffling than one in the centre of a chromosome (Veller et
28 al. 2019). However, almost all previous studies investigating the genetic architecture of recombination
29 rates have focussed solely on autosomal crossover counts (e.g. (Kong et al. 2014; Ma et al. 2015;
30 Johnston et al. 2016; Petit et al. 2017); but see (Brekke et al. 2023). In our study, we modelled both ACC
31 and \bar{r}_{intra} to consider two different (but not necessarily independent) phenomena, that respectively
32 represent more the variation in the mechanistic process of CO formation (ACC) and the variation in
33 crossover positioning and potentially the evolutionary consequences of recombination (\bar{r}_{intra}). We
34 identified a substantial correlation between ACC and \bar{r}_{intra} ($r^2 = 0.684$), reflecting that much of the
35 variation in \bar{r}_{intra} is driven by ACC, whereas the remainder may be due to other factors, such as
36 individual differences in chromatin landscape, differences in the genetic architecture, and/or random
37 processes that affect CO positioning. Females demonstrate higher ACC and \bar{r}_{intra} than males, but this

1 difference is stronger in terms of allele shuffling rather than the number of COs (~1.5x vs 1.37x,
2 respectively). Therefore, females may exhibit a stronger capacity to drive responses to selection than
3 males in this population, although in reality, it may be that the sex-averaged rate is more meaningful in
4 terms of longer term responses to selection (Burt et al. 1991).

5
6 One limitation of our method to characterise COs using pedigree information is that we only use data from
7 gametes that resulted in an offspring. This leads to a “missing fraction” of recombination measures in the
8 population, meaning that our measured rates may not reflect the true rate of crossing over during meiosis;
9 for example, problems in meiosis and lower rates of crossing over can translate into lower fertility and
10 increased rates of aneuploidy in humans (Hassold and Hunt 2001; Kong et al. 2004; Handel and
11 Schimenti 2010; MacLennan et al. 2015). A full understanding of any missing fraction would aim to
12 characterise variation at the pre-zygotic stage e.g. by verifying rate variation using chiasma count data
13 (Malinovskaya, Tishakova, et al. 2020) or gamete sequencing approaches (Dréau et al. 2019) to compare
14 with our pedigree estimated measures. Nevertheless, these methods also have limitations: cytogenetic in
15 birds requires sacrificing individuals to obtain reproductive tissues, and at present, gamete sequencing
16 approaches would be prohibitively expensive to generate large amounts of data (Dréau et al. 2019).
17 Therefore, our pedigree approach is a powerful and useful method to generate large numbers of sex-
18 specific recombination measures (often from pre-existing data in long-term ecological studies).

20 **What is the nature of polygenic variation underpinning recombination rates?**

21 In our study, we show that recombination rates are heritable and present compelling evidence that this
22 variation is polygenic and driven by many loci of small effect. Indeed, the estimate of $h^2 = 0.232$ for
23 female ACC is relatively high compared to other studies of recombination in other vertebrate species
24 (Kong et al. 2014; Johnston et al. 2016; Kadri et al. 2016; Petit et al. 2017; Johnston et al. 2018; Weng et
25 al. 2019; Johnsson et al. 2021; Brekke, Johnston, et al. 2022; Brekke et al. 2023). Our results are similar
26 to mammal studies in that females had higher phenotypic variance and heritability of autosomal crossover
27 counts, but are in contrast in that these studies often identify a conserved suite of loci (e.g. *RNF212*,
28 *RNF212B*, *REC8*, *MSH4*, *HEI10*, among others) that explain a moderate to large effect of heritable
29 variation (e.g. (Kong et al. 2014; Kadri et al. 2016; Petit et al. 2017; Johnston et al. 2018; Brekke, Berg, et
30 al. 2022). A lack of significant GWAS in wild populations is often attributed to reduced power to detect
31 trait loci, due to relatively small sample sizes compared to human and livestock studies (Santure and
32 Garant 2018; Johnston et al. 2022). Our power analysis indicated that a locus would have to contribute
33 >3.2% of the phenotypic variance to be detected, meaning that we would only detect moderate to large
34 effect loci. However, we were able to leverage chromosome partitioning and Empirical Bayes approaches
35 to show strong evidence that the additive genetic variance in recombination rates can be attributed to
36 small effect loci throughout the genome, indicating a polygenic architecture. It remains an open question
37 as to how a polygenic architecture of recombination has influenced its evolution. Nevertheless, the

1 maintenance of polygenic variation can arise due to a number of factors, such as a large mutational target
2 for the introduction of new variants (Rowe and Houle 1996), the distribution of selection coefficients over
3 many loci (Sella and Barton 2019), and/or genomic conflict between linked alleles or unmeasured traits
4 with a similar genetic architecture (Teplitsky et al. 2009; Ruzicka et al. 2019).

5
6 The question remains - how does polygenic variation contribute variation in recombination rate? This trait
7 ultimately is a phenotype of the genome, and polygenic effects will likely operate through two main routes.
8 First, SNPs may be in LD with genomic features that contribute to local regulation of recombination rate
9 variation in *cis*, e.g. via polymorphic hotspots and heritable aspects of chromatin accessibility that are
10 linked to nearby SNPs. Second, SNPs may be in LD with regions of the genome that affect crossover
11 formation in *trans*, e.g. through modifying the cell environment, chromatin structure, and/or the expression
12 and structure of meiotic proteins. It is difficult to directly test *cis* effects in isolation; this could feasibly test
13 if local variation is associated with local recombination rate. However, as crossovers are inherently rare at
14 a localised level, and with a large number of tests to be conducted, this analysis becomes challenging
15 and underpowered. Nevertheless, we were able to test *trans* effects at a global level by adapting the
16 genome partitioning approach to account for recombination rates on chromosomes excluding the focal
17 chromosome. This indicated that male and female \bar{r}_{intra} are likely to be affected by both *cis*- and *trans*-
18 acting polygenic variation, whereas female ACC is largely driven by *trans*-acting polygenic variation.
19 Future work will investigate the correlation of non-zero effect SNPs with functional variation, as well as
20 individual and population fine-scale variation of recombination rate to identify common genomic features
21 within the population.

22
23 Our study has also shown that the female-restricted chromosomes, namely the W and germline-restricted
24 chromosome (GRC), are likely to make a negligible *trans*-acting contribution to heritable variation in
25 recombination rates within each sex. The GRC is present in all passerines and can comprise around 10%
26 of the genome, but is not present in somatic cells (Pigozzi and Solari 1998; Warren et al. 2010;
27 Torgasheva et al. 2019; Borodin et al. 2022). In males, it is generally ejected before meiosis, whereas in
28 females it duplicates and forms crossovers with itself (Malinovskaya, Zadesenets, et al. 2020; Pei et al.
29 2022). The function and evolution of the GRC is still poorly understood, but recent work in blue tits
30 (*Cyanistes caeruleus*) has shown that it is enriched for meiotic genes associated with the synaptonemal
31 complex, although its gene content may differ between species (Kinsella et al. 2019; Mueller et al. 2023).
32 Whilst genetic variation on these chromosomes could not be captured by the SNP array (as this only
33 targets somatic genomes), the dense sparrow pedigree allowed us to solve this question by fitting
34 matriline as a random effect. Whilst a negligible effect is likely true in our study population, we cannot rule
35 out that the W or GRC contributes to variation in recombination rate in other systems.

36
37

1 **Trends and comparisons in linkage mapping and broad-scale recombination landscapes.**

2 Our motivation for constructing a linkage map was to ensure that the SNPs were correctly positioned
3 relative to one another, as any wrongly positioned SNPs could lead to false calling of crossovers. Our
4 higher-density linkage maps showed strong concordance with a previous 6.5K map in the same
5 population (Hagen et al. 2020). There is an expectation that our higher-density map will have improved
6 resolution at telomeric regions and micro-chromosomes to pick up more COs where recombination rates
7 tend to be higher, and more power to detect double crossovers, leading to longer linkage maps. Contrary
8 to our expectation, the male and female maps were shorter in the current study (~90% of the previous
9 estimates; Table S1). This is likely due to the use of Lep-MAP3 in the current study, which is less
10 sensitive to phasing or genotyping errors through design (Rastas 2017) compared to the Cri-MAP
11 software (Green et al. 1990) used in the previous study, where such errors can lead to an inflation of the
12 linkage map length. Both studies also use different mapping functions (Morgan vs Kosambi in the current
13 and previous studies, respectively); however, differences in map distances between these functions are
14 negligible in high-density maps, and as marker densities increase, recombination frequencies can be
15 underestimated relative to map distance, which may also explain the observed patterns (Kivikoski et al.
16 2023).

17
18 Our map confirmed heterogeneity in the recombination landscape, particularly between the sexes, where
19 some regions showed strong divergence in rates (e.g. at ~45Mb on chromosome 1A, or 15-17.5Mb on
20 chromosome 10, among others; Figures S1 and S2). These sex differences indicate that sudden changes
21 in landscape are not necessarily indicative of rearrangements (i.e., when the other sex does not show the
22 same trend), but they could indicate the positions of broader landscape features where males and
23 females can have pronounced heterochiasmy (i.e., differences in male and female rates). Future work will
24 investigate how recombination rate variation, particularly between the sexes, is associated with genomic
25 features. Our overall sex-averaged recombination rate of ~1.98 cM/Mb was concordant with
26 recombination rates estimated based on cytogenetic analysis of chiasma counts and recombination
27 nodules in birds, which range from 1.6 cM/Mb in female common terns (*Sterna hirundo*, (Lisachov et al.
28 2017) to 2.9 cM/Mb in female domestic geese (*Anser anser*, (Torgasheva and Borodin 2017); see data
29 compiled in (Malinovskaya et al. 2018) and Table S1). There is less concordance with previous linkage
30 maps in other species, particularly with those carried out with low marker densities in the early days of
31 linkage mapping, where cM map lengths could be as low as 694 cM for e.g. male Siberian jays (Jaari et
32 al. 2009). It is likely that marker densities in these cases have led to underestimation of recombination by
33 having low sub-telomeric coverage of markers, low sample sizes, and/or markers being too widely spaced
34 to quantify double crossovers. Therefore, understanding how landscapes of recombination vary relative to
35 other avian species requires generation and standardisation of higher density linkage maps in a wider
36 range of systems (Kivikoski et al. 2023).

37

1 **CONCLUSIONS**

2 In this study, we have revealed sex differences in the rate and the genetic architecture of recombination
3 in wild house sparrows. This study is an important step in investigating the selective and evolutionary
4 importance of recombination in wild birds, with future analyses focussing on the effects of crossover
5 interference and association between recombination rates and fitness effects at the individual level.
6 Future work will also benefit from a more nuanced understanding of fine-scale variation in recombination
7 from population-scaled estimates, gamete sequencing, and other molecular approaches (Johnston 2024).
8 Integrating this information with our current dataset may shed light on the potential molecular
9 mechanisms underpinning the distribution of recombination (including both crossover and gene-
10 conversion events) and the specific genomic features associated with local variation in heterochiasmy.
11 Overall, our results expand our understanding of individual variation in recombination in a non-mammal
12 system, and our approach has the potential to be extended to other long-term studies with genomic,
13 pedigree, and fitness information.

14

15 **Material and Methods**

16

17 **Study system.**

18 All data was collected from the meta-population of house sparrows inhabiting an 18-island archipelago
19 covering 1600 km² off the Helgeland coast in Northern Norway (midpoint of 66°32'N, 12°32'E), which has
20 been subject to an individual-based long-term study since 1993 (Jensen et al. 2004). Birds are routinely
21 captured and individually marked from the beginning of May to the middle of August and for
22 approximately one month in the autumn using mist nets (adults and fledged juveniles), or as fledglings in
23 accessible nests during the breeding season. A small (25 µl) blood sample is collected from the brachial
24 vein for DNA from every captured bird. Individual hatch year was determined as either (a) the first year
25 recorded for nestlings or fledged juveniles captured in the summer and autumn, or (b) the year prior to
26 first year recorded for birds first captured as female adults before June 1 or as males before August 1, or
27 (c) a range including the year first recorded and the year prior for birds first captured as adult females
28 after June 1 or adult males after August 1; hatch island is also recorded alongside hatch year (Ranke et
29 al. 2021; Saatoglu et al. 2021). Sampling was conducted in strict accordance with permits from the
30 Norwegian Food Safety Authority and the Ringing Centre at Stavanger Museum, Norway.

31

32 **SNP genotyping and Quality Control.**

33 All SNPs used in our analysis were taken from two custom house sparrow Axiom SNP arrays (200K and
34 70K) based on the resequencing of 33 individual house sparrows (Lundregan et al. 2018). SNPs on both
35 arrays are distributed across 29 autosomes in the house sparrow genome (chromosome 16 was excluded
36 as sequences on this chromosome are difficult to assemble due to containing the highly repetitive major
37 histocompatibility complex). All SNPs on the 70K array are present on the 200K array. All SNP positions

1 are given relative to the house sparrow genome assembly *Passer_domesticus*-1.0 (GenBank Assembly
2 GCA_001700915.1; (Elgvin et al. 2017; Lundregan et al. 2018)). A total of 3,116 recruited adults were
3 successfully genotyped on the 200K array (Niskanen et al. 2020), and an additional 9,079 recruited adults
4 and non-recruited fledglings and juveniles were successfully genotyped on the 70K array. For our
5 analyses, we merged the two datasets using *--bmerge* in PLINK v1.90b7 (Chang et al. 2015), and
6 removed individuals and SNPs with call rates of < 0.1 (using *--mind* and *--geno*) and SNPs with minor
7 allele frequencies (MAF) of < 0.01 in founder individuals (*--maf*). The merged dataset contained 65,840
8 SNPs in 12,965 individuals.

9
10 For all autosomal SNPs used in the estimation of recombination rates below, we conducted a second,
11 stricter round of quality control to minimise the risk of genotypic and/or phasing errors leading to spurious
12 calls of recombination events. Mendelian errors were identified with the *--mendel* function in PLINK, and
13 SNPs with more than 100 Mendelian mismatches were discarded. It is possible that these mismatches
14 have arisen due to DSB repair via biased gene conversion events (Lorenz and Mpaulo 2022); however,
15 as this study only considers crossover events, there is no loss of relevant information by conducting this
16 quality control step. We generated summary statistics of SNP loci using the function *summary.snp.data* in
17 GenABEL v1.8-0 (Aulchenko et al. 2007) in R v3.6.3. To ensure strong concordance between 200K and
18 70K data, we removed SNPs where there was a difference between the datasets of more than 3 standard
19 deviations between (i) the minor allele frequency, (ii) deviation from Hardy-Weinberg equilibrium, and/or
20 (iii) the proportion of heterozygote individuals. After these steps, we retained 56,767 autosomal SNPs and
21 617 Z-linked SNPs in 12,959 individuals. The mean and median autosomal inter-marker distances in this
22 final dataset were 16.1 kb and 9.6 kb, respectively, and the mean and median Z-chromosome inter-
23 marker distances were 111.2 kb and 77.9 kb, respectively. We investigated the linkage disequilibrium
24 (LD) exponential decay profile for all autosomal loci occurring within 500 kb windows using the flag *--ld-*
25 *window-kb 500* in PLINK. LD decayed to $r^2 = 0.01$ at a distance of ~ 100 kb (Figure S7).

26 27 **Genetic pedigree construction.**

28 A metapopulation-level pedigree was constructed using a subset of 873 SNP markers in the software
29 Sequoia (Huisman 2017). This subset of SNPs was selected for the pedigree construction by filtering the
30 70K SNP set using PLINK 1.9 (Chang et al. 2015) using the *--indep* command, specifying a window size
31 of 1000 KB, step size of 10Kb and an r^2 threshold of 0.01, whilst filtering for $MAF > 0.35$ and excluding Z-
32 chromosome mapped SNPs. The SNP set was further refined by constructing a preliminary parentage-
33 only pedigree, and removing SNPs with Mendelian error rates > 0.03 . After these steps, 873 SNPs
34 remained. For genetic sex assignment, we calculated the *Fhat2* inbreeding coefficients (F_z) using the *--*
35 *ibc* command using 306 high-quality Z-chromosome SNPs. Individuals with $F_z > 0.95$ were assigned as
36 female and those with $F_z < 0.5$ assigned as male. Individuals with $F_z > 0.5 < 0.95$ and were left as
37 “unknown” sex, as were individuals assigned as genetic females that had autosomal $F_{ROH} > 0.1$, due to

1 inbreeding biasing F_z estimates. We used the R-package Sequoia (Huisman 2017) to construct a
2 pedigree including 11,073 individuals sampled from Helgeland and several other nearby populations. We
3 used the genetic sex for all individuals and assigned known hatch years as the year of first capture for
4 individuals sampled as nestlings or first captured as juveniles, and assumed sparrows first captured as
5 female adults before June 1 or as males before August 1 were hatched the previous year. We set a
6 possible hatch year range of year $t-1$ or t for sparrows first captured as adult females after June 1 or adult
7 males after August 1 in year t , because by this stage some juveniles are difficult to distinguish from
8 adults. After the initial parentage-only pedigree, a final pedigree was constructed with sib-ship clustering
9 and LLR calculation enabled, with a maximum of eight sib-ship iterations and a genotyping error rate of
10 0.002 (Niskanen *et al.* 2020).

11
12 **Linkage map construction.**
13 Autosomal linkage map construction was conducted using Lep-MAP v3 (Rastas 2017). The pedigree was
14 ordered into full-sib families as follows: for each unique male-female mating pairing (hereafter referred to
15 as the focal individuals, or FIDs, in which meiosis took place), we constructed a three-generation family
16 including all genotyped parents and offspring. Whilst an FID can be present in several families (i.e., as an
17 offspring, parent, or when mating with a different individual), this design meant that each meiosis was
18 only counted once. A total of 4,534 full-sib families were constructed, with 1 to 20 offspring per family. We
19 assumed the same marker order as the house sparrow genome above, and treated each chromosome as
20 a separate linkage group. The module *filtering2* was run with the parameter *datatolerance* = 0.01 to filter
21 based on segregation distortion, with all markers passing this step. The module *separatechromosomes2*
22 was run for each linkage group, and markers that were not assigned to the main group (i.e., LOD score <
23 5) were excluded (N = 2 SNPs removed). Finally, the module *ordermarkers2* was run to calculate the
24 centiMorgan (cM) positions using the Morgan mapping function for each sex separately. Relationships
25 between (a) chromosome length (in megabases) and linkage map length (in cM) and (b) male and female
26 linkage map lengths (in cM) were analysed using linear regressions in R v4.2.2.

27
28 **Calculating individual recombination rates.**
29 **Chromosome phasing and crossover estimation:**
30 The software YAPP v0.2a0 (<https://yapp.readthedocs.io/>) (Servin 2021) was used to phase chromosomes
31 and identify crossover (CO) positions in gametes transmitted from FIDs to their offspring. This approach
32 uses the whole pedigree rather than the smaller sub-pedigrees above, and is more robust to missing
33 individuals, allowing us to characterise crossovers in more individual gametes. YAPP identified 14,769
34 parent-offspring pairs, representing 14,769 gametes in which COs could potentially be inferred. First, the
35 *mendel* command was run with default parameters, removing 143 pairs with higher rates of Mendelian
36 errors using the default parameters. Next, the *phase* command was used to infer the gametic phase of
37 chromosomes. The *phase* analysis proceeds in two stages through the pedigree, ensuring parents are

1 processed before their offspring. In the first stage, Mendelian transmission rules are applied to
2 reconstruct the gametes passed from parent to offspring (e.g., a homozygous individual can only transmit
3 one of the two alleles to its offspring). With this information, the phase of an individual (i.e., the haplotypes
4 received from each parent) is determined by (i) combining all haplotypes transmitted to its offspring using
5 the Weighted Constraints Satisfaction method of (Favier et al. 2010) implemented in ToulBar2 and (ii) the
6 haplotypes transmitted by its parents. In the second stage, the partially reconstructed gametes are used
7 to infer segregation indicators with a Hidden Markov Model, as described in (Fledel-Alon et al. 2011) and
8 (Druet and Georges 2015). These segregation indicators allow for a more precise reconstruction of the
9 gametes transmitted from parent to offspring, which is then used to produce the final phase
10 reconstruction for all individuals. Finally, the *recomb* command was run to identify COs from the
11 segregation indicators. For each chromosome and each meiosis, YAPP outputs the start and stop
12 positions of the informative length of the chromosome (i.e., the total region where phase can be inferred
13 for a particular individual from the pedigree, or “coverage”) and the start and stop positions of each
14 crossover interval as determined by the Hidden Markov Model (Figure S4A); this was included to account
15 for the uneven information for CO detection across parent/offspring pairs (e.g. due to variation in
16 inbreeding). This process was run in three iterations of the *phase* and *recomb* commands to allow
17 conservative quality control and minimise the risks of calling false COs:
18

19 **Iteration 1:** After the first iteration, we removed parent-offspring links with > 60 COs per gamete and/or >
20 9 COs on any chromosomes, and removed parents or offspring with an autosomal heterozygosity of <
21 0.36, as this threshold was associated in an uptick in estimated CO counts, suggesting a reduced sample
22 quality and/or increased phasing difficulty (N = 14,127 gametes remaining).
23

24 **Iteration 2:** After the second iteration, we investigated the genomic locations of double crossovers
25 (DCOs) in close proximity (< 3Mb between adjacent CO mid-points). Chromosome 26 had a high number
26 of close DCOs despite its short length (~6.9 Mb) indicating that this chromosome either has many
27 structural variants or is poorly assembled, and so all COs on this chromosome were discarded. We then
28 identified genomic regions enriched for close DCOs by splitting the genome into 100 kb bins and tallying
29 the number of CO window mid-points in each bin. Two regions of the genome showed elevated close
30 DCOs at chromosome ends: these were from 0-3 Mb of chromosome 4; and from 68-69.9 Mb of
31 chromosome 1A (Figure S8). We speculate that these regions have large structural variants (e.g.
32 inversions) and/or rearrangements relative to the reference genome that lead to false calling of DCOs in
33 these regions. In this case, we removed all COs overlapping these two regions from all further analyses.
34 We then removed all parent-offspring links with > 45 COs per gamete and/or > 9 COs on any
35 chromosome, and removed parents and offspring with a SNP call rate of < 0.98 and/or a heterozygosity
36 value outside 3 standard deviations of the mean (N = 13,159 gametes remaining).
37

1 **Iteration 3:** After running for a third iteration, we re-investigated all DCOs in the data. We assumed that
 2 all COs were Class I crossovers and subject to crossover interference (>90% of COs in vertebrates, see
 3 (Pazhayam et al. 2021). Therefore, we also assumed short DCOs were indicative of non-crossover gene-
 4 conversion events, non-interfering Class-II COs, phasing errors, and/or genotyping errors. After visual
 5 examination of the distribution of distances between DCOs to determine an appropriate threshold, we
 6 identified an increase in DCOs occurring within an interval of 2Mb or less. Whilst the distance at which
 7 crossover interference operates in birds is generally unknown, the lack of DCOs on chromosomes less
 8 than 10Mb in length (Figures 2 & 3) indicates that the 2Mb threshold is unlikely to incorporate Class I
 9 COs. Therefore, we removed all COs that were less than 2Mb apart (from the right-hand boundary of the
 10 first CO interval to the left-hand boundary of the second CO interval; Figure S9B). Any gametes with more
 11 than 5 short DCOs were removed. In cases of clustered short COs (i.e., 3 or more adjacent COs that are
 12 separated by distances of 2 Mb or less), 1 CO was called in the case of odd numbers of COs (i.e., a
 13 phase change occurred at either side of the cluster), or 0 COs in the case of even numbers of COs (i.e.,
 14 there was no phase change on either side of the cluster).

15
 16 It should be noted that pedigree-based methods to estimate COs can only identify those present in one of
 17 the four cells resulting from meiosis. For each CO, there will be two recombinant and two non-
 18 recombinant chromatids at that position. Therefore, our CO counts represent a sample of the crossovers
 19 that happened in meiosis I. We assume that each CO is sampled with a 50:50 probability, but we cannot
 20 rule out that meiosis with two or more COs on the same chromosome may be more likely to be co-
 21 inherited on the same chromatid. Therefore, there is an expectation that at least 50% of gametes will
 22 have at least one CO per chromosome due to obligate crossing-over, as each CO per meiosis has a 50%
 23 chance of being observed in the gamete due to Mendelian segregation. We observed that the micro-
 24 chromosomes 21 to 28 had a higher-than-expected number of gametes with no observed COs (>50%;
 25 Figure 3), meaning that not all COs can be detected. Therefore, all COs occurring on these chromosomes
 26 were discarded from downstream analyses. In total, we identified 212,711 COs in 13,056 phased
 27 genotypes from 6,409 gametes from 1,354 unique females and 6,647 gametes from 1,299 unique males.

28 **Recombination rate calculation:**

29 The CO dataset was used to calculate recombination rates in FIDs using two approaches. First, we
 30 determined the autosomal crossover count (ACC) by summing the number of COs per gamete. Second,
 31 we calculated the rate of intra-chromosomal allelic shuffling, \bar{r}_{intra} , which is the probability that two
 32 randomly chosen SNP loci on the same chromosome are uncoupled in meiosis (Veller et al. 2019). This
 33 was defined as:
 34

$$35 \quad \bar{r}_{intra} = \sum_{k=1}^n 2p_k(1-p_k)L_k^2$$

36

1 where for chromosome k , p_k is the proportion of the SNPs inherited from one parent, L_k is its fraction of
 2 the genome length (or gene count), and n is the number of autosomes. In our initial data exploration, we
 3 also quantified \bar{r}_{intra} as a function of individual genes rather than SNP loci (defined as \bar{r}_{gene}). However,
 4 \bar{r}_{intra} and \bar{r}_{gene} were highly correlated (Pearson's correlation $r = 0.948$, $P < 0.001$; Figure S4B) and so
 5 only the \bar{r}_{intra} measure was used in downstream analyses.

7 **Determining Heritability of Recombination Rate.**

8 **Univariate models:** Variance components and the proportion of phenotypic variance in recombination
 9 measures attributed to additive genetic effects (the narrow-sense heritability, h^2) were determined using
 10 an "animal model" fitted by restricted maximum-likelihood in the package ASReml-R v4 (Butler et al.
 11 2009) in R v4.2.2. A genomic relatedness matrix (GRM) based on all autosomal markers was constructed
 12 with GCTA v1.94.1 (Yang, Lee, et al. 2011). The GRM was adjusted for sampling error using the `--grm-`
 13 `adj 0` argument, which assumes the frequency spectra of genotyped and causal loci are similar. Models
 14 were run for ACC and \bar{r}_{intra} in males and females separately. The fixed effect structure included the total
 15 phase coverage from YAPP (the length of the genome that can be phased and therefore within which
 16 crossovers can be detected) and the total phase coverage squared. For models of \bar{r}_{intra} , we fit with and
 17 without ACC as an additional continuous fixed effect, as intra-locus shuffling is a function of the crossover
 18 count, with both measures highly correlated (Pearson's correlation $r = 0.684$, $P < 0.001$; Figure S6A).
 19 Random effects included the additive genetic effect (GRM) and permanent environment effect. The
 20 permanent environment effect is a repeated measures parameter which accounts for constant differences
 21 between individuals over and above the additive genetic effect, which can be generated by differences in
 22 individual environment and condition, long-term effects of critical developmental stages, and dominance
 23 and epistatic genetic effects (Kruuk 2004). A failure to account for this effect can lead to upwardly biased
 24 estimates of the additive genetic effect (Kruuk and Hadfield 2007). Models were also run with a pedigree-
 25 based relatedness matrix calculated using the `ainv` function in ASReml-R, but variance estimates were
 26 highly similar to those from the GRM. Initial models were run with age of the FID in year of gamete
 27 formation (defined as the difference between offspring hatch year and parent hatch year) as a continuous
 28 fixed covariate, and random effects of FID hatch year, FID natal island and offspring hatch year (to
 29 investigate cohort effects and parse apart environment effects) and FID's mother identity (to estimate
 30 maternal effects). However, these effects were estimated as bounded at zero and were not significant in
 31 any models, and so were discarded from further analyses.

32
 33 The heritability of each measure (h^2) was determined as the ratio of the additive genetic variance V_A to
 34 the total phenotypic variance V_P , defined as the sum of random effect variances and the residual variance
 35 as estimated by the animal model, using the equation $h^2 = V_A/V_P$. We also calculated the mean-
 36 standardised additive genetic variance, defined as the evolvability (I_A) using the equation $I_A = V_A/(\bar{x}^2)$,
 37 where \bar{x} is the trait mean. This measure quantifies the expected proportional change per one unit of

1 selection (Hansen et al. 2011). Standard errors of these estimates were derived using the delta method
 2 implemented in the ASReml-R function *vpredict*.

3
 4 **Bivariate models:** Bivariate models were run to determine the additive genetic covariances and
 5 correlations between male and female ACC and \bar{r}_{intra} with total phase coverage as a continuous fixed
 6 effect. The additive genetic correlation, r_A , was calculated without constraint using the CORGH function
 7 (i.e., correlation with heterogeneous variances) in ASReml-R v4. This function also allowed us to run
 8 additional models where r_A was constrained to zero or 0.999 (as a correlation of one cannot be fit by the
 9 software). Significant differences between the observed value and constrained models were tested using
 10 likelihood ratio tests, calculated as 2 times the difference between the model log-likelihoods, distributed
 11 as χ^2_{df} with 1 degree of freedom.

12
 13 The CORGH function reports the heritabilities of traits when unconditional on the genetic values of the
 14 other sex. To confirm this, we also estimated how much of V_A in females was conditional on genetic
 15 values in males (i.e., $V_{A(f|m)}$), using the following equation:

$$V_{A(f|m)} = V_{Af} - (cov_{A(fm)})^2 / V_{Am}$$

16
 17 where V_{Af} and V_{Am} are the additive genetic variance estimates in females and males, respectively, and
 18 $cov_{A(fm)}$ is the additive genetic covariance of the trait between the sexes (Hansen et al. 2003). The
 19 conditional heritability was then calculated as $h^2_{(f|m)} = V_{A(f|m)} / V_P$. The $cov_{A(fm)}$ estimate was obtained
 20 from the same bivariate animal model as above, specifying the US function (i.e., the covariance matrix is
 21 unstructured). This was then repeated for males, conditional on genetic values in females (i.e., $V_{A(m|f)}$).

22
 23 **Potential Contribution of Female-Restricted Chromosomes to Variation:** House sparrows have two
 24 female-restricted chromosomes present in the cell during meiosis I - a haploid germline-restricted
 25 chromosome (GRC; (Pigozzi and Solari 1998; Warren et al. 2010; Torgasheva et al. 2019; Malinovskaya,
 26 Zadesenets, et al. 2020; Borodin et al. 2022; Pei et al. 2022) and the W chromosome. The function and
 27 evolution of the GRC is poorly understood, but recent work in blue tits (*Cyanistes caeruleus*) has shown
 28 that it is enriched for meiotic genes associated with the synaptonemal complex, although its gene content
 29 may differ between species (Kinsella et al. 2019; Mueller et al. 2023). If there is between-individual
 30 genetic variation for recombination rate on the GRC or W chromosomes, this may be partially captured by
 31 the GRM (as related females will carry more genetically similar GRCs and W chromosomes), but *not* by
 32 the SNP array variation above. To determine their potential contribution to additive genetic variation in
 33 recombination, we used the pedigree to determine the matriline identity of each bird (i.e., the path of
 34 inheritance from mother to offspring). Mother identity was known for 83% of birds through direct
 35 observation or inference of unsampled parents from previous pedigree construction in Sequoia (Huisman
 36 2017; Niskanen et al. 2020). We identified 351 unique matrilineal lines for the 1,354 female birds with

1 (i.e., those with more genes) contribute more to the total additive genetic variance, and thus supporting
2 the hypothesis of a polygenic genetic architecture. For each chromosome i , we calculated two GRMs: one
3 for chromosome i and one for all autosomes excluding i . GRMs were determined using GCTA v1.94.1
4 with the same parameters above. We then fit both GRMs in place of the single GRM in the animal model
5 structure above. This allowed us to determine the proportion of variance of the global recombination rate
6 explained by each chromosome. We then investigated the correlation between chromosome i size and
7 the proportion of additive genetic variance explained by chromosome i using a linear regression in R
8 v4.3.1. It should be noted that chromosome partitioning analyses can be biased as a result of
9 heteroscedasticity and censoring (Kemppainen and Husby 2018), as the trait heritability, SNP effect
10 sizes, and their physical location will impact inferences of polygenic architecture (Kemppainen and Husby
11 2018). To quantify the effect of this, we repeated the chromosome partitioning analysis above, but
12 permuting the phenotype values across all individuals within the model. This was done 100 times, due to
13 computational constraints. We compared the permuted data linear regression with the true regression
14 above, identifying little impact of censoring and heteroscedasticity on our current analysis (Figure S10).

15
16 Finally, we adapted the chromosome partitioning approach to determine if genetic variants underpinning
17 recombination rate are more likely to commonly act in *trans* (i.e., they affect the global recombination rate)
18 or *cis* (i.e., they affect the recombination rate on the chromosome on which they are situated). More
19 simply, this investigates the contribution of each chromosome to recombination on the remaining
20 chromosomes. We repeated the analysis above, except for each chromosome i , we calculated the ACC
21 and \bar{r}_{intra} response variables excluding measures from chromosome i . We then investigated the
22 correlation between chromosome i size and the proportion of additive genetic variance explained by
23 chromosome i using a linear regression in R v4.3.1, as above.

24 25 **DATA STATEMENT**

26 The primary data used for this study is archived on Dryad (<https://doi.org/10.5061/dryad.z08kprpb>) and
27 all associated code is archived on GitHub ([https://github.com/susjoh/2024 Sparrow Recomb GWAS](https://github.com/susjoh/2024_Sparrow_Recomb_GWAS)).

28 29 **ACKNOWLEDGEMENTS**

30 We thank students and fieldworkers for help with fieldwork, and the hospitality of inhabitants at the study
31 area in Helgeland who made this study possible. We thank Katie Abson, Jarrod Hadfield, Anna Hewett,
32 Mark Ravinet, Martin Stoffel, Alexander Suh, Anna Torgasheva, and Carl Veller for helpful discussions on
33 many aspects of the study. This work made extensive use of the Ashworth Computing Cluster Co-
34 operative (AC3) hosted at the Institute of Ecology and Evolution, with assistance from Dominik Laetsch,
35 Cei Abreu-Goodger, and Jobran Chebib.

36
37

1 FUNDING

2 The house sparrow field study and genomic resource development was funded by the Research Council
3 of Norway (RCN grant nos. 221956, 274930 and 302619), the RCN's Centres of Excellence funding
4 scheme (grant no. 223257) and The Royal Society (RGF/R1/180090). S.E.J. was funded by a Royal
5 Society University Research Fellowship (UF150448 and URF/R/211008). J.B.M. was funded by a Darwin
6 Trust of Edinburgh PhD studentship.

8 AUTHOR CONTRIBUTIONS

9 SEJ & HJ conceived and designed the study. HJ and THR organised and collected field data together
10 with AH, HAB and IJH. HAB, HJ, AH, IJH & AKN generated and curated the genomic dataset. HAB &
11 AKN constructed the pedigree. BS developed and adapted YAPP software for the analysis. JBM, CB, LP
12 & SEJ analysed the data. SEJ & JBM wrote the manuscript with input from all authors.

13
14

15 Referenced Literature

- 16
17 Anderson TR. 2006. *Biology of the Ubiquitous House Sparrow: From Genes to Populations*. Oxford, UK:
18 Oxford University Press.
- 19 Araya-Ajoy YG, Niskanen AK, Froy H, Ranke PS, Kvalnes T, Rønning B, Le Pepke M, Jensen H, Ringsby
20 TH, Saether B-E, et al. 2021. Variation in generation time reveals density regulation as an
21 important driver of pace of life in a bird metapopulation. *Ecol. Lett.* 24:2077–2087.
- 22 Aslam ML, Bastiaansen JWM, Crooijmans RPMA, Vereijken A, Megens H-J, Groenen MAM. 2010. A
23 SNP based linkage map of the turkey genome reveals multiple intrachromosomal rearrangements
24 between the turkey and chicken genomes. *BMC Genomics* 11:647.
- 25 Aulchenko YS, Ripke S, Isaacs A, van Duijn CM. 2007. GenABEL: an R library for genome-wide
26 association analysis. *Bioinformatics* 23:1294–1296.
- 27 Backström N, Karaïskou N, Leder EH, Gustafsson L, Primmer CR, Qvarnström A, Ellegren H. 2008. A
28 gene-based genetic linkage map of the collared flycatcher (*Ficedula albicollis*) reveals extensive
29 synteny and gene-order conservation during 100 million years of avian evolution. *Genetics*
30 179:1479–1495.
- 31 Baker Z, Schumer M, Haba Y, Bashkirova L, Holland C, Rosenthal GG, Przeworski M. 2017. Repeated
32 losses of PRDM9-directed recombination despite the conservation of PRDM9 across vertebrates.
33 *Elife* [Internet] 6. Available from: <http://dx.doi.org/10.7554/elife.24133>
- 34 Bascón-Cardozo K, Bours A, Manthey G, Pruisscher P, Durieux G, Dutheil J, Odenthal-Hesse L,
35 Liedvogel M. 2022. Fine-scale map reveals highly variable recombination rates associated with
36 genomic features in the European blackcap. Available from:
37 <http://dx.doi.org/10.22541/au.165423614.49331155/v1>
- 38 Baudat F, Buard J, Grey C, Fledel-Alon A, Ober C, Przeworski M, Coop G, de Massy B. 2010. PRDM9 is
39 a major determinant of meiotic recombination hotspots in humans and mice. *Science* 327:836–
40 840.

- 1 Borodin P, Chen A, Forstmeier W, Fouché S, Malinovskaya L, Pei Y, Reifová R, Ruiz-Ruano FJ,
2 Schlebusch SA, Sotelo-Muñoz M, et al. 2022. Mendelian nightmares: the germline-restricted
3 chromosome of songbirds. *Chromosome Res.* 30:255–272.
- 4 Brandvain Y, Coop G. 2012. Scrambling eggs: meiotic drive and the evolution of female recombination
5 rates. *Genetics* 190:709–723.
- 6 Brekke C, Berg P, Gjuvsland AB, Johnston SE. 2022. Recombination rates in pigs differ between breeds,
7 sexes and individuals, and are associated with the RNF212, SYCP2, PRDM7, MEI1 and MSH4
8 loci. *Genet. Sel. Evol.* 54:33.
- 9 Brekke C, Johnston SE, Gjuvsland AB, Berg P. 2022. Variation and genetic control of individual
10 recombination rates in Norwegian Red dairy cattle. *J. Dairy Sci.* [Internet]. Available from:
11 <http://dx.doi.org/10.3168/jds.2022-22368>
- 12 Brekke C, Johnston SE, Knutsen T, Berg P. 2023. Genetic architecture of individual meiotic crossover
13 rate and distribution in a large Atlantic Salmon (*Salmo salar*) breeding population. *BioRxiv*
14 [Internet]. Available from: <http://dx.doi.org/10.1101/2023.06.07.543993>
- 15 Burt A, Bell G, Harvey PH. 1991. Sex differences in recombination. *J. Evol. Biol.* 4:259–277.
- 16 Butler DG, Cullis BR, Gilmour AR, Gogel BJ. 2009. Mixed models for S language environments: ASReml-
17 R Reference Manual.
- 18 Calderón PL, Pigozzi MI. 2006. MLH1-focus mapping in birds shows equal recombination between sexes
19 and diversity of crossover patterns. *Chromosome Res.* 14:605–612.
- 20 Capilla L, Medarde N, Alemany-Schmidt A, Oliver-Bonet M, Ventura J, Ruiz-Herrera A. 2014. Genetic
21 recombination variation in wild Robertsonian mice: on the role of chromosomal fusions and
22 Prdm9 allelic background. *Proc. Biol. Sci.* 281:20140297.
- 23 Cattani MV, Kingan SB, Presgraves DC. 2012. Cis- and trans-acting genetic factors contribute to
24 heterogeneity in the rate of crossing over between the *Drosophila simulans* clade species. *J.*
25 *Evol. Biol.* 25:2014–2022.
- 26 Chan AH, Jenkins PA, Song YS. 2012. Genome-wide fine-scale recombination rate variation in
27 *Drosophila melanogaster*. *PLoS Genet.* 8:e1003090.
- 28 Chang CC, Chow CC, Tellier LC, Vattikuti S, Purcell SM, Lee JJ. 2015. Second-generation PLINK: rising
29 to the challenge of larger and richer datasets. *Gigascience* 4:7.
- 30 Charlesworth B, Barton NH. 1996. Recombination load associated with selection for increased
31 recombination. *Genet. Res.* 67:27–41.
- 32 Cirulli ET, Kliman RM, Noor MAF. 2007. Fine-scale crossover rate heterogeneity in *Drosophila*
33 *pseudoobscura*. *J. Mol. Evol.* 64:129–135.
- 34 Cooney CR, Mank JE, Wright AE. 2021. Constraint and divergence in the evolution of male and female
35 recombination rates in fishes. *Evolution* 75:2857–2866.
- 36 Coop G, Przeworski M. 2007. An evolutionary view of human recombination. *Nature Reviews Genetics*
37 [Internet] 8:23–34. Available from: <http://dx.doi.org/10.1038/nrg1947>
- 38 Devlin B, Roeder K. 1999. Genomic control for association studies. *Biometrics* 55:997–1004.
- 39 Dréau A, Venu V, Avdievich E, Gaspar L, Jones FC. 2019. Genome-wide recombination map
40 construction from single individuals using linked-read sequencing. *Nat. Commun.* 10:4309.

- 1 Druet T, Georges M. 2015. LINKPHASE3: an improved pedigree-based phasing algorithm robust to
2 genotyping and map errors. *Bioinformatics* 31:1677–1679.
- 3 Elgvin TO, Trier CN, Tørresen OK, Hagen IJ, Lien S, Nederbragt AJ, Ravinet M, Jensen H, Sætre G-P.
4 2017. The genomic mosaicism of hybrid speciation. *Sci. Adv.* 3:e1602996.
- 5 Favier A, Elsen J-M, de Givry S, Legarra A. 2010. Optimal haplotype reconstruction in half-sib families. In:
6 ICLP-10 workshop on Constraint Based Methods for Bioinformatics. Available from:
7 <http://dx.doi.org/10.29007/rpn1>
- 8 Felsenstein J. 1974. The evolutionary advantage of recombination. *Genetics* 78:737–756.
- 9 Fledel-Alon A, Leffler EM, Guan Y, Stephens M, Coop G, Przeworski M. 2011. Variation in human
10 recombination rates and its genetic determinants. *PLoS One* 6:e20321.
- 11 Garagna S, Page J, Fernandez-Donoso R, Zuccotti M, Searle JB. 2014. The Robertsonian phenomenon
12 in the house mouse: mutation, meiosis and speciation. *Chromosoma* 123:529–544.
- 13 Green P, Falls K, Crooks S. 1990. Documentation for CRIMAP, Version 2.4. Washington University
14 School of Medicine, St. Louis, MO
- 15 Grey C, Baudat F, de Massy B. 2018. PRDM9, a driver of the genetic map. *PLoS Genet.* 14:e1007479.
- 16 Groenen MAM, Wahlberg P, Foglio M, Cheng HH, Megens H-J, Crooijmans RPMA, Besnier F, Lathrop M,
17 Muir WM, Wong GK-S, et al. 2009. A high-density SNP-based linkage map of the chicken
18 genome reveals sequence features correlated with recombination rate. *Genome Res.* 19:510–
19 519.
- 20 Hagen IJ, Lien S, Billing AM, Elgvin TO, Trier C, Niskanen AK, Tarka M, Slate J, Saetre G-P, Jensen H.
21 2020. A genome-wide linkage map for the house sparrow (*Passer domesticus*) provides insights
22 into the evolutionary history of the avian genome. *Mol. Ecol. Resour.* 20:544–559.
- 23 Halldorsson BV, Palsson G, Stefansson OA, Jonsson H, Hardarson MT, Eggertsson HP, Gunnarsson B,
24 Oddsson A, Halldorsson GH, Zink F, et al. 2019. Characterizing mutagenic effects of
25 recombination through a sequence-level genetic map. *Science* 363:eaau1043.
- 26 Handel MA, Schimenti JC. 2010. Genetics of mammalian meiosis: regulation, dynamics and impact on
27 fertility. *Nat. Rev. Genet.* 11:124–136.
- 28 Hansen TF, Pélabon C, Armbruster WS, Carlson ML. 2003. Evolvability and genetic constraint in
29 *Dalechampia* blossoms: components of variance and measures of evolvability. *J. Evol. Biol.*
30 16:754–766.
- 31 Hansen TF, Pélabon C, Houle D. 2011. Heritability is not Evolvability. *Evol. Biol.* 38:258–277.
- 32 Hansson B, Akesson M, Slate J, Pemberton JM. 2005. Linkage mapping reveals sex-dimorphic map
33 distances in a passerine bird. *Proc. Biol. Sci.* 272:2289–2298.
- 34 Hansson B, Ljungqvist M, Dawson DA, Mueller JC, Olano-Marin J, Ellegren H, Nilsson J-A. 2010. Avian
35 genome evolution: insights from a linkage map of the blue tit (*Cyanistes caeruleus*). *Heredity*
36 (*Edinb.*) 104:67–78.
- 37 Hassold T, Hunt P. 2001. To err (meiotically) is human: the genesis of human aneuploidy. *Nature*
38 *Reviews Genetics* [Internet] 2:280–291. Available from: <http://dx.doi.org/10.1038/35066065>
- 39 Hill WG, Robertson A. 1966. The effect of linkage on limits to artificial selection. *Genetical Research*
40 [Internet] 8:269–294. Available from: <http://dx.doi.org/10.1017/s0016672300010156>

- 1 Hinch R, Donnelly P, Hinch AG. 2023. Meiotic DNA breaks drive multifaceted mutagenesis in the human
2 germ line. *Science* 382:eadh2531.
- 3 Huisman J. 2017. Pedigree reconstruction from SNP data: parentage assignment, sibship clustering and
4 beyond. *Mol. Ecol. Resour.* 17:1009–1024.
- 5 Hunter CM, Huang W, Mackay TFC, Singh ND. 2016. The genetic architecture of natural variation in
6 recombination rate in *Drosophila melanogaster*. *PLoS Genet.* 12:e1005951.
- 7 Jaari S, Li M-H, Merilä J. 2009. A first-generation microsatellite-based genetic linkage map of the Siberian
8 jay (*Perisoreus infaustus*): insights into avian genome evolution. *BMC Genomics* 10:1.
- 9 Jensen H, SAEther B-E, Ringsby TH, Tufto J, Griffith SC, Ellegren H. 2004. Lifetime reproductive success
10 in relation to morphology in the house sparrow *Passer domesticus*. *J. Anim. Ecol.* 73:599–611.
- 11 Johnsson M, Whalen A, Ros-Freixedes R, Gorjanc G, Chen C-Y, Herring WO, de Koning D-J, Hickey JM.
12 2021. Genetic variation in recombination rate in the pig. *Genet. Sel. Evol.* 53:54.
- 13 Johnston SE. 2024. Understanding the Genetic Basis of Meiotic Recombination Variation: Past, Present
14 and Future. *Mol. Biol. Evol.* 41:msae112.
- 15 Johnston SE, Bérénois C, Slate J, Pemberton JM. 2016. Conserved Genetic Architecture Underlying
16 Individual Recombination Rate Variation in a Wild Population of Soay Sheep (*Ovis aries*).
17 *Genetics* 203:583–598.
- 18 Johnston SE, Chen N, Josephs EB. 2022. Taking Quantitative Genomics into the Wild. *Proc. Roy. Soc. B*
19 289:20221930.
- 20 Johnston SE, Huisman J, Pemberton JM. 2018. A Genomic Region Containing REC8 and RNF212B Is
21 Associated with Individual Recombination Rate Variation in a Wild Population of Red Deer
22 (*Cervus elaphus*). *G3* 8:2265–2276.
- 23 Kadri NK, Harland C, Faux P, Cambisano N, Karim L, Coppieters W, Fritz S, Mullaart E, Baurain D,
24 Boichard D, et al. 2016. Coding and noncoding variants in HFM1, MLH3, MSH4, MSH5, RNF212,
25 and RNF212B affect recombination rate in cattle. *Genome Res.* 26:1323–1332.
- 26 Kawakami T, Mugal CF, Suh A, Nater A, Burri R, Smeds L, Ellegren H. 2017. Whole-genome patterns of
27 linkage disequilibrium across flycatcher populations clarify the causes and consequences of fine-
28 scale recombination rate variation in birds. *Mol. Ecol.* 26:4158–4172.
- 29 Kawakami T, Smeds L, Backström N, Husby A, Qvarnström A, Mugal CF, Olason P, Ellegren H. 2014. A
30 high-density linkage map enables a second-generation collared flycatcher genome assembly and
31 reveals the patterns of avian recombination rate variation and chromosomal evolution. *Mol. Ecol.*
32 23:4035–4058.
- 33 Kempainen P, Husby A. 2018. Inference of genetic architecture from chromosome partitioning analyses
34 is sensitive to genome variation, sample size, heritability and effect size distribution. *Mol. Ecol.*
35 *Resour.* 18:767–777.
- 36 Kinsella CM, Ruiz-Ruano FJ, Dion-Côté A-M, Charles AJ, Gossman TI, Cabrero J, Kappei D, Hemmings
37 N, Simons MJP, Camacho JPM, et al. 2019. Programmed DNA elimination of germline
38 development genes in songbirds. *Nat. Commun.* 10:5468.
- 39 Kivikoski M, Rastas P, Löytynoja A, Merilä J. 2023. Predicting recombination frequency from map
40 distance. *Heredity (Edinb.)* 130:114–121.

- 1 Koehler KE, Hawley RS, Sherman S, Hassold T. 1996. Recombination and nondisjunction in humans and
2 flies. *Hum. Mol. Genet.* 5 Spec No:1495–1504.
- 3 Kondrashov AS. 1988. Deleterious mutations and the evolution of sexual reproduction. *Nature* 336:435–
4 440.
- 5 Kong A, Barnard J, Gudbjartsson DF, Thorleifsson G, Jonsdottir G, Sigurdardottir S, Richardsson B,
6 Jonsdottir J, Thorgeirsson T, Frigge ML, et al. 2004. Recombination rate and reproductive
7 success in humans. *Nat. Genet.* 36:1203–1206.
- 8 Kong A, Thorleifsson G, Frigge ML, Masson G, Gudbjartsson DF, Vilmoes R, Magnusdottir E,
9 Olafsdottir SB, Thorsteinsdottir U, Stefansson K. 2014. Common and low-frequency variants
10 associated with genome-wide recombination rate. *Nat. Genet.* 46:11–16.
- 11 Kruuk LEB. 2004. Estimating genetic parameters in natural populations using the “animal model.” *Philos.*
12 *Trans. R. Soc. Lond. B Biol. Sci.* 359:873–890.
- 13 Kruuk LEB, Hadfield JD. 2007. How to separate genetic and environmental causes of similarity between
14 relatives. *J. Evol. Biol.* 20:1890–1903.
- 15 Kumar S, Suleski M, Craig JM, Kasparowicz AE, Sanderford M, Li M, Stecher G, Hedges SB. 2022.
16 TimeTree 5: An expanded resource for species divergence times. *Mol. Biol. Evol.* [Internet] 39.
17 Available from: <http://dx.doi.org/10.1093/molbev/msac174>
- 18 Lenormand T. 2003. The evolution of sex dimorphism in recombination. *Genetics* 163:811–822.
- 19 Lenormand T, Dutheil J. 2005. Recombination difference between sexes: a role for haploid selection.
20 *PLoS Biol.* 3:e63.
- 21 Lisachov AP, Malinovskaya LP, Druzyaka AV, Borodin PM, Torgasheva AA. 2017. Synapsis and
22 recombination of autosomes and sex chromosomes in two terns (Sternidae, Charadriiformes,
23 Aves). *Vavilovskii Zhurnal Genet. Seleksii* 21:259–268.
- 24 Lorenz A, Mpaulo SJ. 2022. Gene conversion: a non-Mendelian process integral to meiotic
25 recombination. *Heredity (Edinb.)* 129:56–63.
- 26 Lundregan SL, Hagen IJ, Gohli J, Niskanen AK, Kemppainen P, Ringsby TH, Kvalnes T, Pärn H, Rønning
27 B, Holand H, et al. 2018. Inferences of genetic architecture of bill morphology in house sparrow
28 using a high-density SNP array point to a polygenic basis. *Mol. Ecol.* 27:3498–3514.
- 29 Ma L, O’Connell JR, VanRaden PM, Shen B, Padhi A, Sun C, Bickhart DM, Cole JB, Null DJ, Liu GE, et
30 al. 2015. Cattle Sex-Specific Recombination and Genetic Control from a Large Pedigree Analysis.
31 *PLoS Genet.* 11:e1005387.
- 32 MacLennan M, Crichton JH, Playfoot CJ, Adams IR. 2015. Oocyte development, meiosis and aneuploidy.
33 *Semin. Cell Dev. Biol.* 45:68–76.
- 34 Malinovskaya L, Shnaider E, Borodin P, Torgasheva A. 2018. Karyotypes and recombination patterns of
35 the Common Swift (*Apus apus* Linnaeus, 1758) and Eurasian Hobby (*Falco subbuteo* Linnaeus,
36 1758). *Avian Res.* [Internet] 9. Available from: <http://dx.doi.org/10.1186/s40657-018-0096-7>
- 37 Malinovskaya LP, Tishakova K, Shnaider EP, Borodin PM, Torgasheva AA. 2020. Heterochiasmy and
38 sexual dimorphism: The case of the barn swallow (*Hirundo rustica*, hirundinidae, Aves). *Genes*
39 (*Basel*) 11:1119.
- 40 Malinovskaya LP, Zadesenets KS, Karamysheva TV, Akberdina EA, Kizilova EA, Romanenko MV,
41 Shnaider EP, Scherbakova MM, Korobitsyn IG, Rubtsov NB, et al. 2020. Germline-restricted

- 1 chromosome (GRC) in the sand martin and the pale martin (Hirundinidae, Aves): synopsis,
2 recombination and copy number variation. *Sci. Rep.* 10:1058.
- 3 Mank JE. 2009. The evolution of heterochiasmy: the role of sexual selection and sperm competition in
4 determining sex-specific recombination rates in eutherian mammals. *Genet. Res. (Camb.)*
5 91:355–363.
- 6 Mueller JC, Schlebusch SA, Pei Y, Poignet M, Vontzou N, Ruiz-Ruano FJ, Albrecht T, Reifová R,
7 Forstmeier W, Suh A, et al. 2023. Micro germline-restricted chromosome in blue tits: Evidence for
8 meiotic functions. *Mol. Biol. Evol.* [Internet] 40. Available from:
9 <http://dx.doi.org/10.1093/molbev/msad096>
- 10 Muñoz-Fuentes V, Marcet-Ortega M, Alkorta-Aranburu G, Linde Forsberg C, Morrell JM, Manzano-
11 Piedras E, Söderberg A, Daniel K, Villalba A, Toth A, et al. 2015. Strong artificial selection in
12 domestic mammals did not result in an increased recombination rate. *Mol. Biol. Evol.* 32:510–
13 523.
- 14 Myers S, Bottolo L, Freeman C, McVean G, Donnelly P. 2005. A fine-scale map of recombination rates
15 and hotspots across the human genome. *Science* 310:321–324.
- 16 Myers S, Bowden R, Tumian A, Bontrop RE, Freeman C, MacFie TS, McVean G, Donnelly P. 2010. Drive
17 against hotspot motifs in primates implicates the PRDM9 gene in meiotic recombination. *Science*
18 327:876–879.
- 19 Nei M. 1969. Linkage modifications and sex difference in recombination. *Genetics* 63:681–699.
- 20 Niskanen AK, Billing AM, Holand H, Hagen IJ, Araya-Ajoy YG, Husby A, Rønning B, Myhre AM, Ranke
21 PS, Kvalnes T, et al. 2020. Consistent scaling of inbreeding depression in space and time in a
22 house sparrow metapopulation. *Proc. Natl. Acad. Sci. U. S. A.* 117:14584–14592.
- 23 van Oers K, Santure AW, De Cauwer I, van Bers NEM, Crooijmans RPMA, Sheldon BC, Visser ME, Slate
24 J, Groenen MAM. 2014. Replicated high-density genetic maps of two great tit populations reveal
25 fine-scale genomic departures from sex-equal recombination rates. *Heredity (Edinb.)* 112:307–
26 316.
- 27 Otto SP, Barton NH. 2001. Selection for recombination in small populations. *Evolution* 55:1921–1931.
- 28 Otto SP, Lenormand T. 2002. Resolving the paradox of sex and recombination. *Nat. Rev. Genet.* 3:252–
29 261.
- 30 Pan J, Sasaki M, Kniewel R, Murakami H, Blitzblau HG, Tischfield SE, Zhu X, Neale MJ, Jasin M, Socci
31 ND, et al. 2011. A hierarchical combination of factors shapes the genome-wide topography of
32 yeast meiotic recombination initiation. *Cell* 144:719–731.
- 33 Pazhayam NM, Turcotte CA, Sekelsky J. 2021. Meiotic crossover patterning. *Front. Cell Dev. Biol.*
34 9:681123.
- 35 Pei Y, Forstmeier W, Ruiz-Ruano FJ, Mueller JC, Cabrero J, Camacho JPM, Alché JD, Franke A,
36 Hoepfner M, Börno S, et al. 2022. Occasional paternal inheritance of the germline-restricted
37 chromosome in songbirds. *Proc. Natl. Acad. Sci. U. S. A.* 119:e2103960119.
- 38 Peñalba JV, Deng Y, Fang Q, Joseph L, Moritz C, Cockburn A. 2020. Genome of an iconic Australian
39 bird: High-quality assembly and linkage map of the superb fairy-wren (*Malurus cyaneus*). *Mol.*
40 *Ecol. Resour.* 20:560–578.
- 41 Petit M, Astruc J-M, Sarry J, Drouilhet L, Fabre S, Moreno C, Servin B. 2017. Variation in recombination
42 rate and its genetic determinism in sheep populations. *Genetics* 207:767–784.

- 1 Pigozzi MI. 2001. Distribution of MLH1 foci on the synaptonemal complexes of chicken oocytes.
2 *Cytogenet. Cell Genet.* 95:129–133.
- 3 Pigozzi MI, Solari AJ. 1998. Germ cell restriction and regular transmission of an accessory chromosome
4 that mimics a sex body in the zebra finch, *Taeniopygia guttata*. *Chromosome Res.* 6:105–113.
- 5 Ranke PS, Araya-Ajoy YG, Ringsby TH, Pärn H, Rønning B, Jensen H, Wright J, Saether B-E. 2021.
6 Spatial structure and dispersal dynamics in a house sparrow metapopulation. *J. Anim. Ecol.*
7 90:2767–2781.
- 8 Rastas P. 2017. Lep-MAP3: robust linkage mapping even for low-coverage whole genome sequencing
9 data. *Bioinformatics* 33:3726–3732.
- 10 Ritz KR, Noor MAF, Singh ND. 2017. Variation in recombination rate: Adaptive or not? *Trends Genet.*
11 33:364–374.
- 12 Robledo-Ruiz DA, Gan HM, Kaur P, Dudchenko O, Weisz D, Khan R, Lieberman Aiden E, Osipova E,
13 Hiller M, Morales HE, et al. 2022. Chromosome-length genome assembly and linkage map of a
14 critically endangered Australian bird: the helmeted honeyeater. *Gigascience* [Internet] 11.
15 Available from: <http://dx.doi.org/10.1093/gigascience/giac025>
- 16 Rönnegård L, McFarlane SE, Husby A, Kawakami T, Ellegren H, Qvarnström A. 2016. Increasing the
17 power of genome wide association studies in natural populations using repeated measures -
18 evaluation and implementation. *Methods Ecol. Evol.* 7:792–799.
- 19 Ross-Ibarra J. 2004. The evolution of recombination under domestication: a test of two hypotheses. *Am.*
20 *Nat.* 163:105–112.
- 21 Rowe L, Houle D. 1996. The lek paradox and the capture of genetic variance by condition dependent
22 traits. *Proc. Biol. Sci.* 263:1415–1421.
- 23 Ruzicka F, Hill MS, Pennell TM, Flis I, Ingleby FC, Mott R, Fowler K, Morrow EH, Reuter M. 2019.
24 Genome-wide sexually antagonistic variants reveal long-standing constraints on sexual
25 dimorphism in fruit flies. *PLoS Biol.* 17:e3000244.
- 26 Saatoglu D, Niskanen AK, Kuismin M, Ranke PS, Hagen IJ, Araya-Ajoy YG, Kvalnes T, Pärn H, Rønning
27 B, Ringsby TH, et al. 2021. Dispersal in a house sparrow metapopulation: An integrative case
28 study of genetic assignment calibrated with ecological data and pedigree information. *Mol. Ecol.*
29 30:4740–4756.
- 30 Samuk K, Manzano-Winkler B, Ritz KR, Noor MAF. 2020. Natural selection shapes variation in genome-
31 wide recombination rate in *Drosophila pseudoobscura*. *Curr. Biol.* 30:1517-1528.e6.
- 32 Santure AW, Garant D. 2018. Wild GWAS—association mapping in natural populations. *Mol. Ecol.*
33 *Resour.* 18:729–738.
- 34 Sardell JM, Kirkpatrick M. 2020. Sex differences in the recombination landscape. *Am. Nat.* 195:361–379.
- 35 Sella G, Barton NH. 2019. Thinking About the Evolution of Complex Traits in the Era of Genome-Wide
36 Association Studies. *Annu. Rev. Genomics Hum. Genet.* 20:461–493.
- 37 Servin B. 2021. YAPP: Yet Another Phasing Program. Available from: <https://yapp-doc.netlify.app/>
- 38 Singhal S, Leffler EM, Sannareddy K, Turner I, Venn O, Hooper DM, Strand AI, Li Q, Raney B,
39 Balakrishnan CN, et al. 2015. Stable recombination hotspots in birds. *Science* 350:928–932.

- 1 Smukowski CS, Noor MAF. 2011. Recombination rate variation in closely related species. *Heredity*
2 (*Edinb.*) 107:496–508.
- 3 Stapley J, Birkhead TR, Burke T, Slate J. 2008. A linkage map of the zebra finch *Taeniopygia guttata*
4 provides new insights into avian genome evolution. *Genetics* 179:651–667.
- 5 Stapley J, Feulner PGD, Johnston SE, Santure AW, Smadja CM. 2017. Variation in recombination
6 frequency and distribution across eukaryotes: patterns and processes. *Philos. Trans. R. Soc.*
7 *Lond. B Biol. Sci.* 372:20160455.
- 8 Stephens M. 2017. False discovery rates: a new deal. *Biostatistics* 18:275–294.
- 9 Stubberud MW, Myhre AM, Holand H, Kvalnes T, Ringsby TH, Saether B-E, Jensen H. 2017. Sensitivity
10 analysis of effective population size to demographic parameters in house sparrow populations.
11 *Mol. Ecol.* 26:2449–2465.
- 12 Teplitsky C, Mills JA, Yarrall JW, Merilä J. 2009. Heritability of fitness components in a wild bird
13 population. *Evolution* 63:716–726.
- 14 Torgasheva AA, Borodin PM. 2017. Immunocytological Analysis of Meiotic Recombination in the Gray
15 Goose (*Anser anser*). *Cytogenet. Genome Res.* 151:27–35.
- 16 Torgasheva AA, Malinovskaya LP, Zadesenets KS, Karamysheva TV, Kizilova EA, Akberdina EA,
17 Pristyazhnyuk IE, Shnaider EP, Volodkina VA, Saifitdinova AF, et al. 2019. Germline-restricted
18 chromosome (GRC) is widespread among songbirds. *Proc. Natl. Acad. Sci. U. S. A.* 116:11845–
19 11850.
- 20 Trivers R. 1988. Sex differences in rates of recombination and sexual selection. In: Richard E. Michod
21 BRL, editor. *Evolution of Sex: An Examination of Current Ideas*. Sunderland, Massachusetts:
22 Sinauer Associates Inc. p. 270–286.
- 23 Veller C, Kleckner N, Nowak MA. 2019. A rigorous measure of genome-wide genetic shuffling that takes
24 into account crossover positions and Mendel's second law. *Proc. Natl. Acad. Sci. U. S. A.*
25 116:1659–1668.
- 26 Visscher PM, Wray NR, Zhang Q, Sklar P, McCarthy MI, Brown MA, Yang J. 2017. 10 years of GWAS
27 discovery: Biology, function, and translation. *Am. J. Hum. Genet.* 101:5–22.
- 28 Warren WC, Clayton DF, Ellegren H, Arnold AP, Hillier LW, Künstner A, Searle S, White S, Vilella AJ,
29 Fairley S, et al. 2010. The genome of a songbird. *Nature* 464:757–762.
- 30 Weng Z, Wolc A, Su H, Fernando RL, Dekkers JCM, Arango J, Settar P, Fulton JE, O'Sullivan NP,
31 Garrick DJ. 2019. Identification of recombination hotspots and quantitative trait loci for
32 recombination rate in layer chickens. *J. Anim. Sci. Biotechnol.* 10:20.
- 33 Yang J, Lee SH, Goddard ME, Visscher PM. 2011. GCTA: a tool for genome-wide complex trait analysis.
34 *Am. J. Hum. Genet.* 88:76–82.
- 35 Yang J, Manolio TA, Pasquale LR, Boerwinkle E, Caporaso N, Cunningham JM, de Andrade M, Feenstra
36 B, Feingold E, Hayes MG, et al. 2011. Genome partitioning of genetic variation for complex traits
37 using common SNPs. *Nat. Genet.* 43:519–525.6666

38

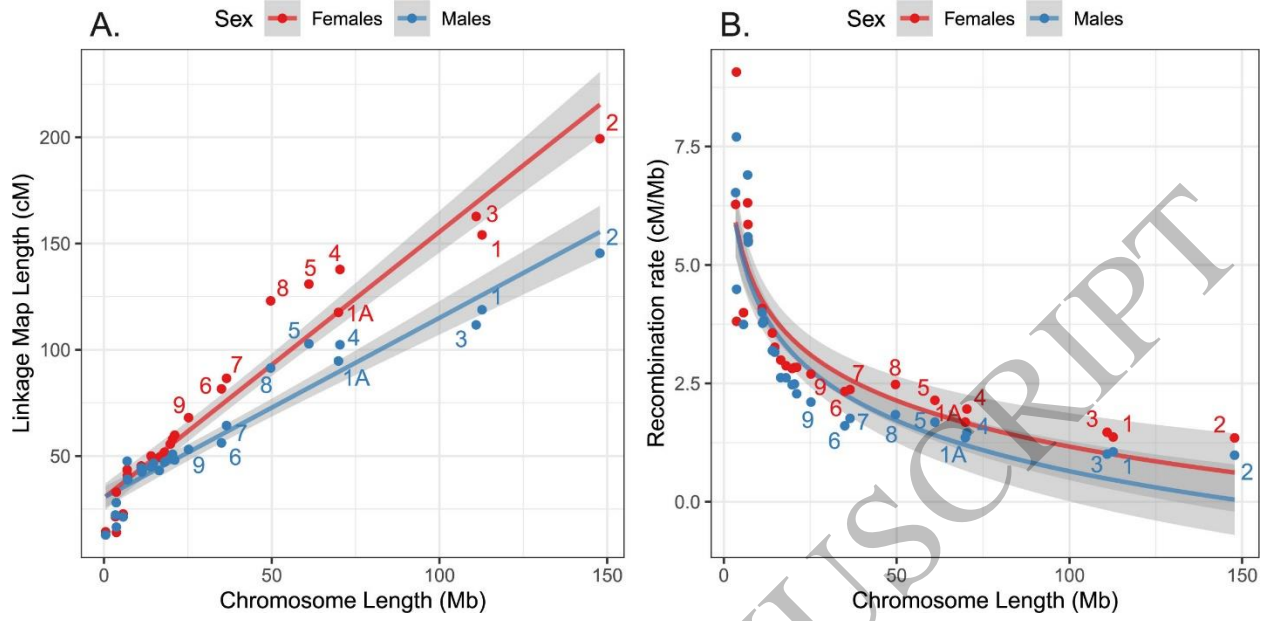


Figure 2
165x81 mm (x DPI)

1

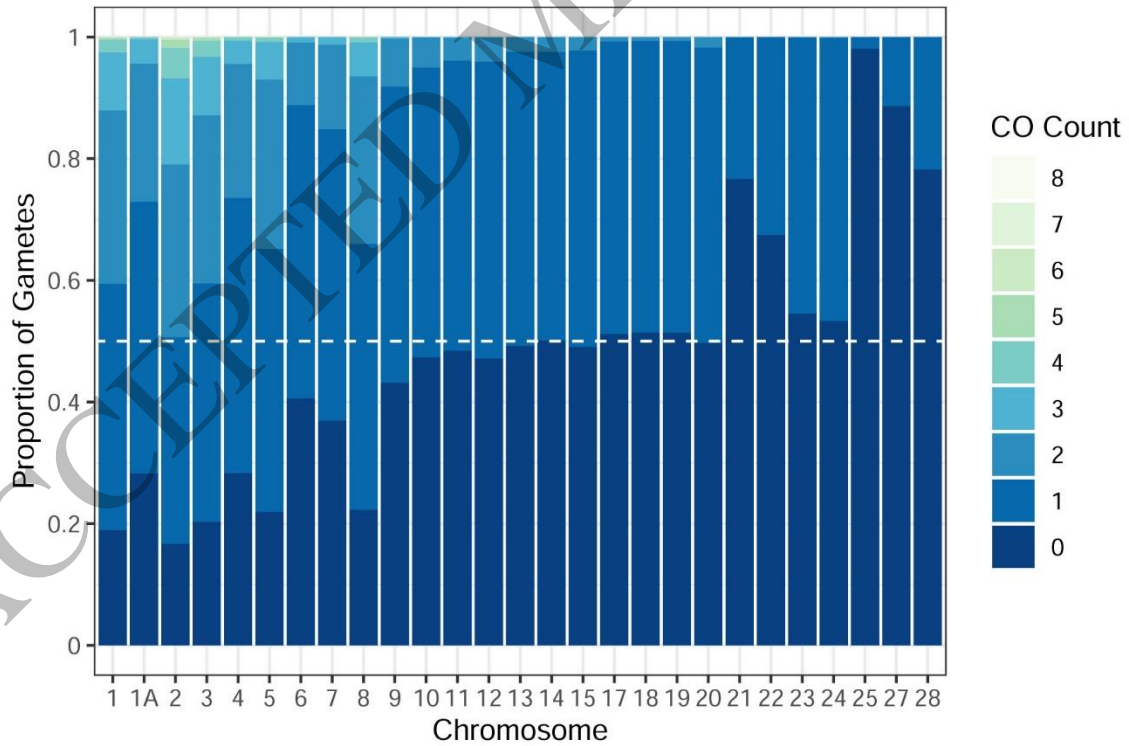


Figure 3
152x102 mm (x DPI)

2

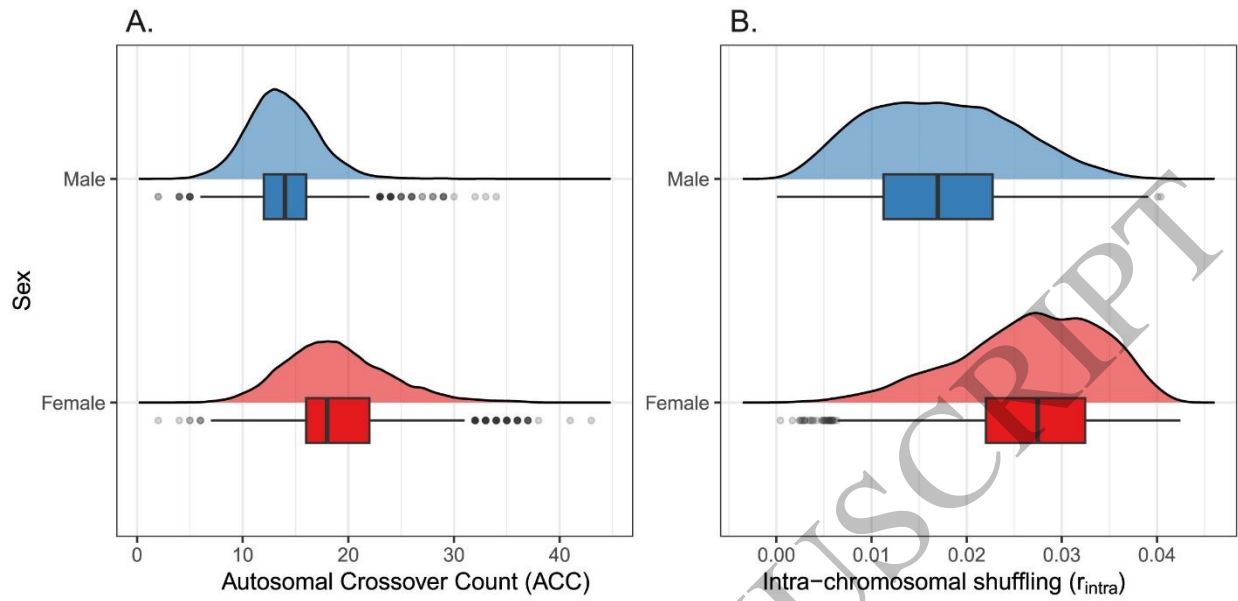


Figure 4
165x83 mm (x DPI)

1

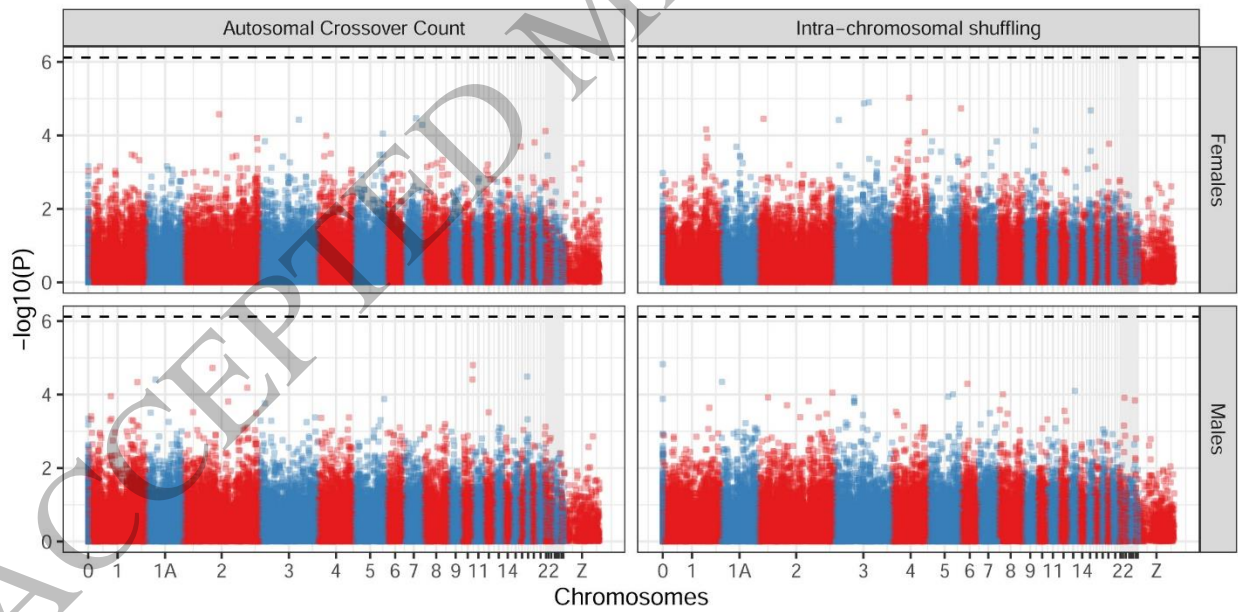


Figure 5
165x83 mm (x DPI)

2

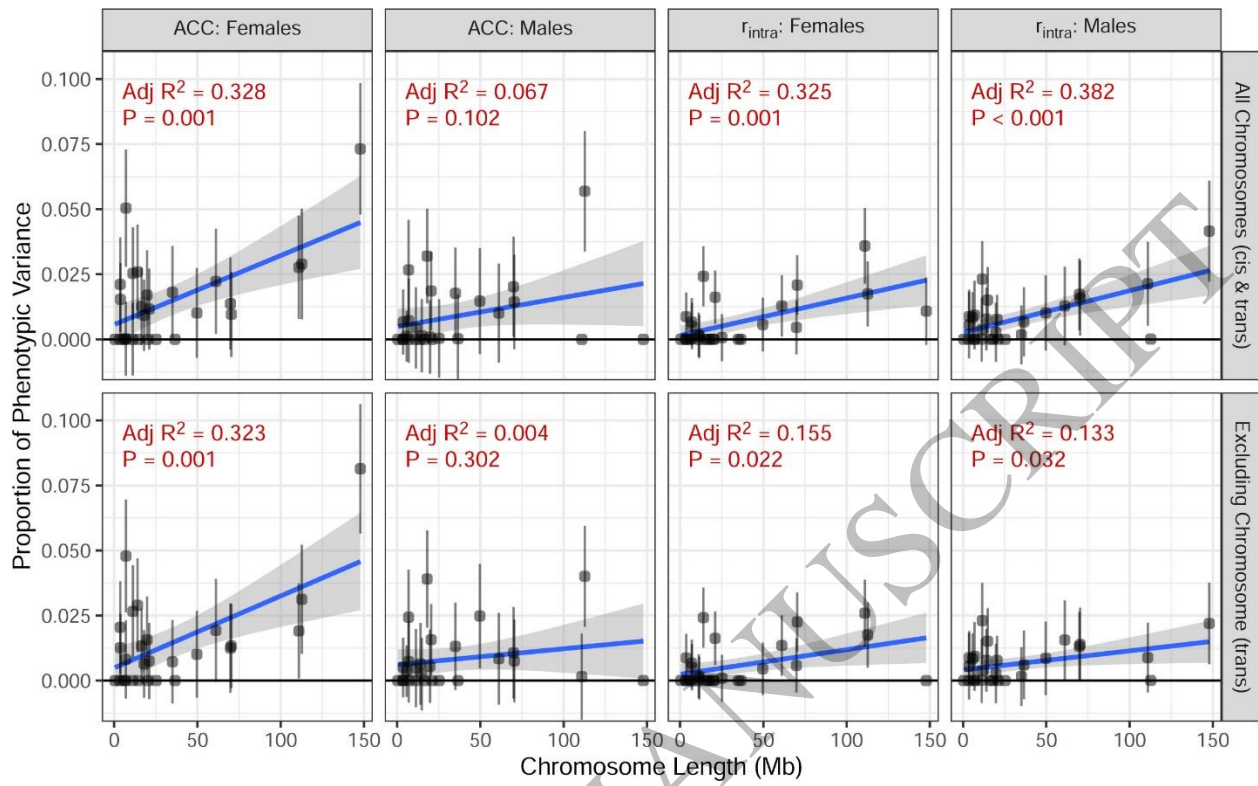


Figure 6
165x102 mm (x DPI)